12-2008

An Integrated Routing and Distributed Scheduling Approach for Hybrid IEEE 802.16E Mesh Networks For Vehicular Broadband Communications

Rahul Amin
Clemson University, ramin@clemson.edu

An Integrated Routing and Distributed Scheduling Approach For Hybrid IEEE 802.16E Mesh Networks For Vehicular Broadband Communications

---

A Dissertation
Presented to
the Graduate School of
Clemson University

In Partial Fulfillment
of the Requirements for the Degree
Master of Science
Computer Engineering

---

by
Rahul N. Amin
December 2008

Accepted by:
Dr. Kuang-Ching Wang, Committee Chair
Dr. Harlan Russell
Dr. Jim Martin

Abstract

An integrated routing and distributed scheduling approach for fast deployable IEEE 802.16e networks is presented where distributed base stations with dual radios form a mesh backhaul and subscriber stations communicate through these base stations. The mesh backhaul is formed via an IEEE 802.16e mesh mode radio on each base station, while the subscriber stations communicate with base stations via PMP mode radios. The proposed routing scheme divides the deployed network into several routing zones. Each routing zone contains several base stations that form the mesh backhaul with one base station equipped with either a fiber, satellite or any other point-to-point backhaul link to reach a gateway on the core network (for example, Internet or Enterprise Network). Traffic from the subscriber stations is routed by the serving base station through the mesh to the gateway-connected base station using min-hop routing metric. Mobile IP scheme is used to assign a care-of address to a subscriber station that moves from one routing zone to the other, thereby avoiding a change in IP address for network layer applications. The scheduling approach consists of two phases. In the first phase, a centralized mesh scheduling algorithm is applied with collected information on network topology, radio parameters, and initial QoS provisioning requirements. At the same time, each base station derives a PMP schedule for actual demands from associated subscriber stations constrained by the initial mesh schedule. In the second phase, each base station monitors its carried PMP traf-

fic load statistics; to accommodate traffic load changes in a distributed fashion, each base station lends or borrows time slots from neighboring base stations to adjust its mesh and PMP radio schedules. The distributed schedule adaptation method not only allows individual base stations to accommodate short-term increases in bandwidth demands, it also provides the means for optimizing the mesh and PMP schedules with respect to actual bandwidth demands. Several deployment strategies are considered and an analytical model is developed to identify the achievable increase in overall network throughput using the proposed scheduling approach. Simulations are run in network simulator ns-2 to verify results obtained using the analytical model.

Dedication

This thesis is dedicated to my beloved family - my mother, my father and my brother. Their support has helped me climb the steps of success in every phase of my life.

Acknowledgments

I would like to thank my advisor, Dr. Kuang-Ching Wang, for all his guidance and motivation. Throughout my undergraduate and graduate studies at Clemson University, he gave me valuable support and advices and has always provided insightful thoughts on research problems that helped me direct my thoughts in the right direction. I would like to thank him for all the valuable knowledge and experience he has shared with me. I appreciate the time we have spent together working on the research issues and driving it towards a meaningful direction.

I would also like to thank Dr. Joachim Taiber and every employee at the BMW IT Research Center in Greenville. The project that I worked on, vehicular mobile broadband connectivity, at the ITRC showed me the practical side of things and always kept me motivated in conducting my research. It also gave me a valuable opportunity to meet with top notch IT professionals in the industry and get their opinion on WiMAX's potential as the next generation mobile broadband technology.

I would also like to thank all the colleagues in the wireless group at Clemson University for their friendship and help. I have had a great time conducting my research and following everyone else's research. It has always been a pleasure to interact with such an intelligent group. I have enjoyed all the time spent with my colleagues in the lab and office.

Table of Contents

List of Tables

List of Figures

Chapter 1

Introduction

WiMAX, an acronym for Worldwide Interoperability for Microwave Access, is the next-generation mobile broadband technology based on IEEE 802.16 family of standards [1], [2]. Mobile WiMAX is based on the IEEE 802.16e-2005 standard [2], which extends mobility support over the earlier IEEE 802.16-2004 [1] standard that supports only fixed stations. The two standards altogether offer a low-cost infrastructure solution [3] for long range, broadband (typically up to 3 miles non-line-of-sight, 6 miles line-of-sight, and 30 Mbps per 10 MHz channel [4]) mobile communications. Typical network deployments include fixed infrastructure deployed along roadside for general vehicular communications and dynamic (semi-nomadic) infrastructure for military vehicular communications.

The IEEE 802.16-2004 and 802.16e-2005 standards together have provided the link layer functions needed to support persistent vehicle communication. Specifically, IEEE 802.16-2004 defines the mesh mode operation that allows construction of a wireless mesh of base stations (BS) to provide continuous coverage for subscriber stations (SS) over a large area, with only a few backhaul-enabled BSs connected to the core network via point-to-point communication links. In mesh mode, BSs maintain

control and data connections of controllable bandwidth with neighboring BSs. IEEE 802.16e-2005 provides the definition of a mobile station (MS) and its network entry, scheduling, and BS handover procedures. The mobility extension was defined in the point-to-multipoint (PMP) mode but was not defined to interoperate with BSs in mesh mode. To enable persistent MS communication with a BS mesh, coordination of the two modes of operation with higher layer protocols must be defined.

A number of studies have examined the feasibility of adopting WiMAX and/or Mobile WiMAX for constructing a last-mile tactical network for the mobile warfighters. In [5], communications among base commands and non-mobile branch units using IEEE 802.16-2001 (WiMAX specification for operation in 10 to 66 GHz frequency range) was studied. In [6], link-level performance assessments were done for communications between a moving vehicle and a single fixed base station using IEEE 802.16-2004. In [7], a solution for enabling mesh and ad hoc networking using the IEEE 802.16-2004 PMP mode was studied. The modifications in the frame structure presented in the proposed solution made WiMAX conducive to the construction of mobile ad-hoc networks (MANETs). In [8], operational needs of a last mile tactical network and the WiMAX standards potentials in meeting them were discussed, concluding that the current technology as defined in the standards [1], [2] can satisfy near-term last-mile broadband connectivity requirements while additional specifications still need to be developed to support long-term tactical wireless communication networks. For warfighters on the move, of crucial need is sustained reliable communication with the commands over a tactical network infrastructure. This thesis investigates the required network organization, message routing, and link layer scheduling methods for enabling persistent communication of fast moving vehicles over a Mobile WiMAX mesh network.

In this thesis, a strategy is proposed to support persistent vehicle commu-

nication (for commercial vehicular or tactical military networks) with a standard-compliant Mobile WiMAX mesh network. A tactical military network is made up of several mobile warfighters on the battlefield transmitting/receiving data to/from a central base-command core network. The tactical network operation involves a mesh of BSs deployed along potential paths that the MSs travel. Amidst a majority of mesh BSs (MSS), a few backhaul-enabled BSs (MBS) with point-to-point links to the core network gateway are deployed. Each MS upon network entry instantiates network connections with the nearest base station, and the connections persist across subsequent BS handovers. The persistence is enabled at the link and network layer, respectively, by the Mobile WiMAX handover support and the proposed integrated routing and scheduling methods.

The proposed routing method exploits the coverage continuity of the wireless mesh infrastructure to achieve communication persistence. Within the mesh, end-to-end routes between an MS and the core network adapt according to the movement pattern of each MS. The packets within the mesh are routed through one or more BSs using min-hop criteria till it reaches a backhaul-enabled BS. Once reaching the backhaul-enabled BS, packets are routed using Mobile IP and globally addressed routing protcols, e.g. ad hoc routing protocols. MS mobility events are signaled to the scheduling service to control migration of existing connection types to neighboring BSs, and to initiate adaptations in the global routing protocol.

The proposed scheduling method uses distributed adaptation in conjunction with initial centralized algorithm to improve the overall network throughput performance. A centralized algorithm proposed in [9] derives near-optimal-throughput transmission schedules for a WiMAX mesh network considering spectral reuse opportunities and known aggregate traffic demands at each node. In [10], for supporting different WiMAX service classes at a single base station, a two-level scheduling so-

lution for OFDM networks is proposed which generates the schedule for different service classes first (macro-step) and then generates the schedule for traffic within each scheduled service class (micro-step). The proposed scheduling solution combines these concepts in two steps. First, when a new BS joins the mesh, e.g., when a tactical network is being deployed, each MBS in the field utilizes a centralized algorithm to derive an initial schedule for all BSs in its intra-gateway routing zone. At the same time, each base station derives a PMP schedule for actual demands from associated mobile stations subject to the initial mesh schedule capacity. Since the actual traffic load to be serviced by each BS is unknown initially, each BS is assumed to have a uniform load for deriving the initial schedule. Then, once the initial schedule is assigned, the network enters the operational phase, during which each BS coordinates with other BSs in its two-hop neighborhood to dynamically adjust its schedule.

An analytical model is derived to verify the increase in overall network throughput using the proposed network architecture, routing protcol, and scheduling solutions. Simulations are run in ns-2 to complement the analytical model, showing a throughput enhancement of as high as 232% for one of the simulated topologies using the distributed adaptation approach over the centralized-only scheduling approach. The rest of the thesis is organized as follows. Chapter 2 reviews relevant background on WiMAX standards and previous studies of centralized and distributed schedulers. Chapter 3 describes the studied network model. Chapter 4 describes the proposed routing protocol. Chapter 5 describes the proposed scheduling solution. An analytical model for two deployment strategies is derived in Chapter 6. Simulation studies and results to verify the analytical model are also presented in Chapter 6. The paper concludes in Section 7 and future work is identified.

Chapter 2

Background and Related Work

2.1 WiMAX PMP and Mesh Modes

The IEEE 802.16-2004 standard defines the mesh mode as an option beyond the default PMP mode [1]. The PMP mode allows MSS to communicate only through a BS. The PMP mode can utilize one of three physical layers: orthogonal frequency-division multiplexing (OFDM), orthogonal frequency-division multiple access (OFDMA), and a single carrier modulation scheme. In mesh mode, SSs can communicate with any other SSs in range as well, thereby allowing SSs to relay packets to or from other SSs. In mesh context, a backhaul-enabled node is referred to as a Mesh BS, and all other nodes (including MSs as later defined in IEEE 802.16e [2]) are called Mesh SSs. The mesh mode is only supported by OFDM modulation according to the standard. Through contention-based procedures during network entry, all nodes establish frame-based, contention-free schedules for data transmission. The schedules can be assigned by a Mesh BS for all dependent SSs using a centralized scheduling scheme (e.g., [9],[11],[12]), or be collaboratively determined by all nodes using a distributed scheduling scheme (e.g., [13]). PMP and mesh modes also

have important differences in their supported duplex schemes and frame structures. PMP mode supports both time-division-duplex (TDD) and frequency-division-duplex (FDD) while mesh mode supports TDD only. In PMP mode, frames are separated for uplink and downlink traffic, while in mesh mode frames are separated for control and data traffic regardless of direction. In [7] and [14], efforts were made to realize the mesh mode frames under PMP mode operation. A more detailed description of both PMP and Mesh mode OFDM frame structure is given in Section 2.1.1 and Section 2.1.2 respectively. Additional information on PMP frame formats using OFDMA and single carrier modulation schemes can be found in [1], [15].

In both PMP and mesh modes, a SS must enter the network by connecting with a BS or, in mesh mode, with another SS following a network entry procedure that: 1) scans for and synchronizes to the node to be connected to, and then performs 2) ranging, 3) basic capabilities negotiation, 4) authorization, 5) registration, 6) IP address configuration, 7) time of day configuration, and 8) provisioned connections setup with the connected node. The two modes differ in their exchanged messages during steps 1 to 3, while the remaining steps are the same. The network entry procedure is closely relevant to the handover latency. As described in Section 2.2, steps 1 and 2 are essential for a MS to restore basic communications with a new BS, while all other steps may be bypassed if the BSs share the existing states of the MS.

Data is always transmitted contention-free on WiMAX links. Contention-free transmission opportunities must be setup prior to data transmission in the form of connections. In PMP mode, five types of provisioned service connections of controlled bandwidths can be instantiated to provide different quality of service levels. The five service types are: Unsolicited Grant Service (UGS), Real-time Polling Service (rtPS), Non-real-time Polling Service (nrtPS), Best Effort (BE), and Extended real-time Polling Service (ertPS) [3]. In mesh mode, only one mesh connection is created

between two neighboring nodes. Quality of service differentiation is on a packet by packet basis. Bandwidth of each mesh connection, as mentioned, is determined with a centralized or distributed scheduling scheme.

2.1.1 WiMAX Point-to-Multipoint Mode Frame Format

In PMP mode, a BS communicates with several MSs in its range. Data is exchanged between a BS and each MS in a structured fixed length frame format. Figure 2.1 shows an overview of the PMP mode frame format. The BS scheduler is in charge of dividing up the frame such that a contention-free transmission schedule is obtained. Based on various parameters such as channel bandwidth, modulation scheme, coding rate, cyclic prefix and uplink-to-downlink traffic ratio, the BS scheduler determines how much uplink traffic and downlink traffic it can support. The BS can estimate the uplink-to-downlink traffic demand ratio and divide the PMP mode frame into proportionate uplink and downlink sub-frames. The uplink and downlink sub-frames are further divided into data bursts (minislots) of varied length. Each MS that a BS communicates with might have different traffic requirements. Based on the demand from each associated MS, the BS scheduler can assign the data bursts to different MSs in both the uplink and downlink direction. The information regarding the assignment of minislots (schedule) is broadcasted by the BS in the first downlink burst in each frame in form of UL-MAP and DL-MAP messages.

2.1.2 WiMAX Mesh Mode Frame Format

In mesh mode, any Mesh base station (MBS) or Mesh subscriber station (MSS) can talk to any other MBS or MSS directly. Data is exchanged between nodes in a structured fixed length frame format. Figure 2.2 shows an overview of the mesh

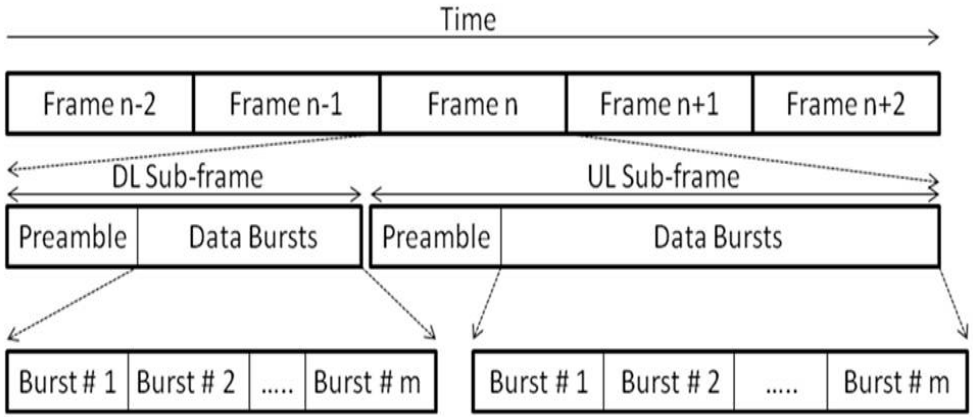

Figure 2.1: PMP Mode OFDM Frame Structure

mode OFDM frame format. For communication between two neighboring nodes, only one mesh connection is created. There is neither service class differentiation nor is the mesh mode frame divided into uplink and downlink sub-frames. The mesh mode frame is divided into control and data sub-frames instead. The control sub-frame can be assigned to either schedule control or network control messages. Each control sub-frame contains mini-slots of equal length that are capable of transmitting 7 OFDM symbols. The number of mini-slots in the sub-frame depends on variable MSH_CTRL_LEN which is related to the number of BSs in the mesh. The schedule control sub-frame which supports both central and distributed scheduling messages is used to come up with a contention-free transmission schedule. If a centralized scheduling scheme is used, the MBS is in charge of coming up with a contention-free transmission schedule. For a distributed scheduling scheme, two-hop neighbors communicate to reach a mutually agreed upon schedule. A combination of the two schemes can also be used to accomplish the same task. According to the determined schedule, different number of data sub-frame minislots are assigned to different nodes to send their traffic bursts.

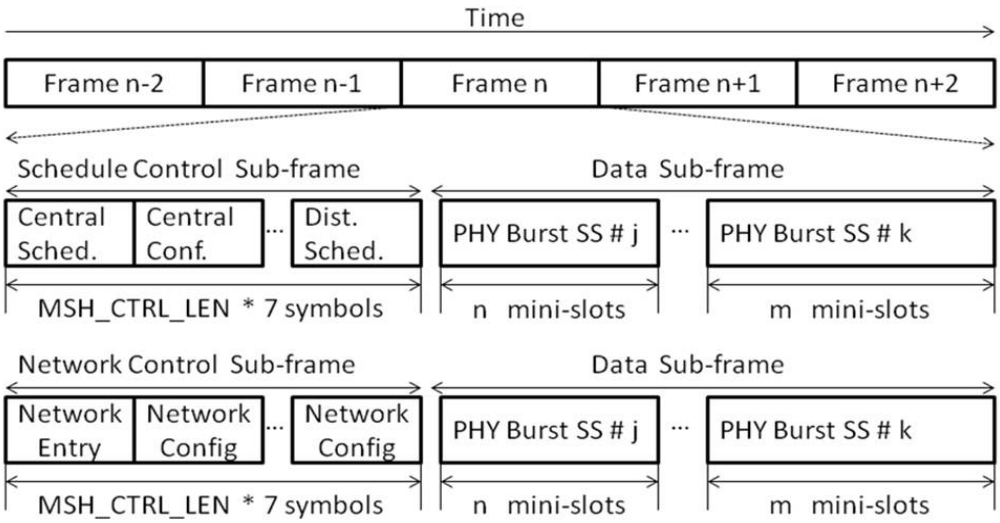

Figure 2.2: Mesh Mode OFDM Frame Structure

2.2 Mobile WiMAX Extension

The IEEE 802.16e-2005 standard extends the IEEE 802.16-2004 standard by specifying MS-specific functions, primarily concerning MS handover across base stations. The handover functions are, however, defined for PMP mode only. In PMP mode, BSs can advertise a list of target BSs based on network topology, while each MS can also scan for neighboring BSs for inclusion in its own target BSs list. Each MS maintains up-to-date CINR (carrier-to-interference-and-noise ratio) from the serving BS as well as scanned neighboring BSs, based on which either an MS or a BS can decide to initiate a handover process. Default handover procedure starts with either an MS sending a handover request to the serving BS or, vice versa, a BS sending a handover request to the MS. In either case, the MS decides the target BS to switch to, sends a handover indication message to the serving BS, and starts synchronizing with the target BS. The handover process can repeat the full network entry procedure, or be shortened to as little as two steps (synchronizing and ranging), provided the

previous BS forwards all current connection states of the MS to the new BS.

Two more fast handover options are specified: macro-diversity handover (MDHO) and fast base station switching (FBSS). With either option, the MS and the serving BS maintain a list of neighboring BSs called the Diversity Set. MDHO is essentially a soft-handover method, with all BSs in the Diversity Set transmitting the same message in the same frequency at the same time, while an MS receives all transmissions as one. Vice versa, all BS's in the set simultaneously receive messages transmitted by the MS. FBSS is a hard handover method. An MS communicates with only one BS at a time, while it can handover to any BS in the Diversity Set with even less effort than the fastest standard handover procedure. That is, an MS sends to the serving BS either a standard handover request message over the control connection or a predefined codeword over a pre-allocated fast-feedback channel, and then it can synchronize with the target BS. The MDHO/FBSS options do have a downside by requiring all BSs to operate in the same frequency channel and transmit in synchronized time frames, rendering very limited network capacity and scheduling flexibility.

2.3 Related Work

Several researchers have investigated WiMAX scheduling solutions for increasing a WiMAX mesh network's throughput. In [9],[16], [17], the authors propose a centralized interference-aware mesh scheduling solution to increase the overall network capacity. In [9], a cross-layer tree-based routing algorithm along with interference aware scheduling is proposed where stations are allowed to transmit following the order of highest transmission demand which results in a near-optimal overall network throughput performance. In [16], a load-aware routing and a two-step scheduling solution are proposed where proportional time-slots based on traffic demands at each

subscriber are allocated separately for interfering and non-interfering frame duration. The separation of interfering and non-interfering frame allocation exploits spectral reuse capability of any mesh topology and thus supports higher traffic demand from each subscriber station in the mesh. In [17], the improvement in overall network throughput by considering a mesh link between two nodes as bidirectional instead of a separated uplink and downlink portion during interference-aware transmission schedule construction is presented.

In [13], a stochastic model for distributed mesh scheduling, when aggregate traffic demands are known, is presented which provides fairness, bandwidth guarantees, and good channel utilization. This solution does not consider different WiMAX service class priorities. In [10], a two-step QoS scheduling scheme for single base station OFDM networks is presented where utility functions based on delay-sensitive and non-delay sensitive applications are defined to maximize user satisfaction. In the first step, the utility function of traffic is defined, according to which the scheduling order of different services is determined. In the second step, scheduling is done among all users of the same service type determined in the first step.

Several other studies evaluate the performance of various WiMAX scheduling algorithms operating in the PMP mode. In [18], four different scheduling schemes (first-in-first-out, earliest due date, preemptive earliest due date, and transmission opportunity based scheduling) are considered and performance in terms of mean delay and average system throughput is studied. Transmission opportunity based scheduling has been shown to outperform the other four scheduling schemes. In [19], a technique to compensate for channel errors using CINR information is proposed to preserve QoS and fairness of a WF2Q+ based scheduling algorithm. Simulation studies in ns-2 were carried out to verify results. In [20], the authors evaluate throughput, delay and loss rate performance of six different scheduling approaches which include

droptail, fair queuing, weighted fair queuing, deficit round robin, random early detection, and random early detection with in/out. Simulations are done in ns-2 to peform the analysis. In [21], the authors derive sufficient conditions for a set of scheduled grants to be allocated so that the transmission of each half-duplex SS does not overlap with its reception. They formally prove the properties of these conditions and then demonstrate its effectiveness in carrying a mix of VOIP and Web traffic via simulations. Several other studies ([22], [23], [24]) provide a similar performance analysis for various scheduling approaches to be used with WiMAX PMP mode.

The centralized algorithm proposed in [9] derives near-optimal-throughput transmission schedules for a WiMAX mesh network considering spectral reuse opportunities and known aggregate traffic demands at each node. Different service class priorities are not considered in this work. In [10], a strategy to differentiate traffic based on different service classes is presented. The initial centralized mesh scheduling solution proposed in this thesis combines the strategies provided in these two papers to achieve near-optimal-throughput transmission schedule while differentiating traffic based on service class priorities. The PMP mode scheduling solution proposed in this thesis is based on first-in-first-out concept with different service class priorities taken into consideration.

Chapter 3

Network Architecture

The network model considered in this thesis is illustrated in Figure 3.1. The network is built with a number of BSs deployed along pathways in a tactical military environment and is connected to the core network via a number of backhaul-enabled BSs (e.g., via satellite links). The BSs are configured in mesh mode, such that the backhaul-enabled BSs are Mesh BSs, and all other BSs are Mesh SSs. Mobile stations are fast moving vehicles traversing the pathways in either direction. To maintain persistent communication on the move, the vehicles are to be MSs communicating with and handing over across the BSs along the path. The MSs and BSs, therefore, must be operated in the PMP mode to leverage the mobility support. To fulfill this network model, each BS is equipped with dual radios, one operated in mesh mode and the other in PMP mode, while each MS is equipped with one PMP mode radio. The protocol architecture for the BSs and MSs is shown in Figure 3.2.

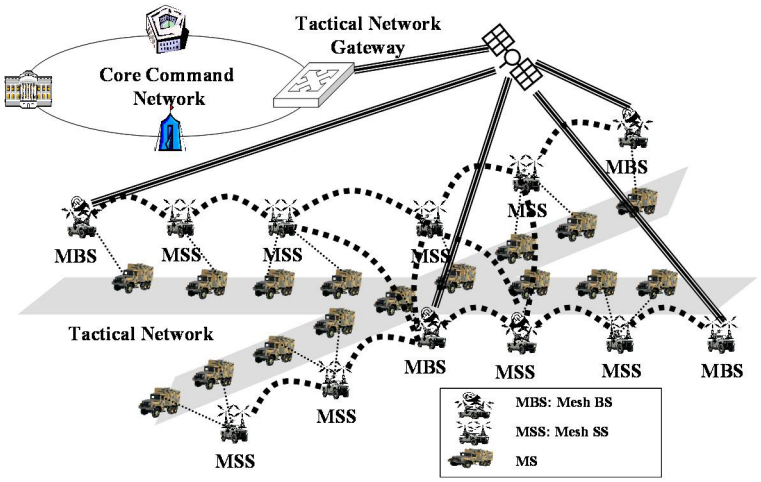

Figure 3.1: The Proposed Protcol Architecture

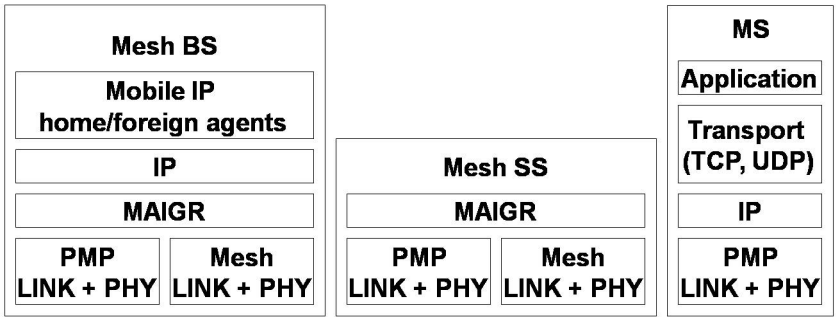

Figure 3.2: BS (MBS, MSS) and MS Protcol Architecture

3.1 Base Station Communication

All BSs, Mesh BSs and Mesh SSs, participate in mesh construction with their mesh mode radios. From a Mesh SS's perspective, its mesh radio provides a multi-hop backhaul connection to the core network. The mesh connectivity is established upon deployment, and the mesh topology depends on the BSs positions and their transmit power. Bandwidth of each mesh connection is negotiated upon deployment. The proposed centralized scheduling with distributed adaptation scheme is implemented at the link layer for this purpose. The mesh routing agent on each BS mesh radio implements the proposed Mobility-Aware Intra-Gateway Routing (MAIGR) protocol as described in Section 4. The Mesh BSs are gateways to the core command network, which is assumed to be a classical or ad hoc IP network, for which the Mesh BSs shall support its respective routing protocols. To support seamless IP mobility, Mobile IP is assumed to be supported. Each Mesh BS implements Mobile IP home-agent and foreign-agent services, and a dynamic host configuration protocol (DHCP) service for assigning MS addresses upon their entry. A distinct range of IP addresses is allocated for use at each BS, and each assigned MS address is assumed to be timed out after long durations of inactivity (no messages destined for an MS or no periodic presence indication sent from an MS).

3.2 Mobile Station Communication

MSs communicate through a BS in range using their PMP radios. Upon network entry, each MS acquires three control connections and one data connection with the initial BS. The MS specifies one among the five provisioned services and the desired bandwidth for its data connection. All connections, once instantiated, will

persist across handovers until the MSs request to terminate them. Each MS address, once assigned, also persists until the MS exits the network and the address timeouts un-refreshed. Persistent transport protocol connections, such as TCP connections, are enabled with BS-supported Mobile IP, BS-supported full-state handover, and the proposed MAIGR protocol.

Chapter 4

Routing Protocol

Message routing is accomplished in two separate domains. Exterior to the Mesh BSs is an IP-based core network. Routing in the exterior domain is done with existing IP routing protocols and Mobile IP deployed at the Mesh BSs. Interior to the Mesh BSs is the intra-gateway mesh domain. Routing in the mesh domain is based on the MAIGR protocol in separate intra-gateway routing zones. An intra-gateway routing zone is defined with respect to each Mesh BS, enclosing the Mesh BS and all Mesh SSs that declare the Mesh BS as their gateway. Typically but not necessarily, a Mesh SS declares a closest Mesh BS to be its gateway. Figure 4.1 demonstrates the routing zone terminology pictorially.

Originally defined in [25], Mobile IP utilizes home agents to assign home addresses to MSs and foreign agents to assign care-of addresses for MSs entering a new network. A home agent is typcially located at the gateway for a MS's home network where the MS has acquired its home address. The home agent always caches the most recent incoming packets for an MS in a limited-size buffer. Once a MS enters a new network, it registers with a foreign agent, who assigns to the MS a care-of address and notifies its home agent of the care-of address. Once informed, the home

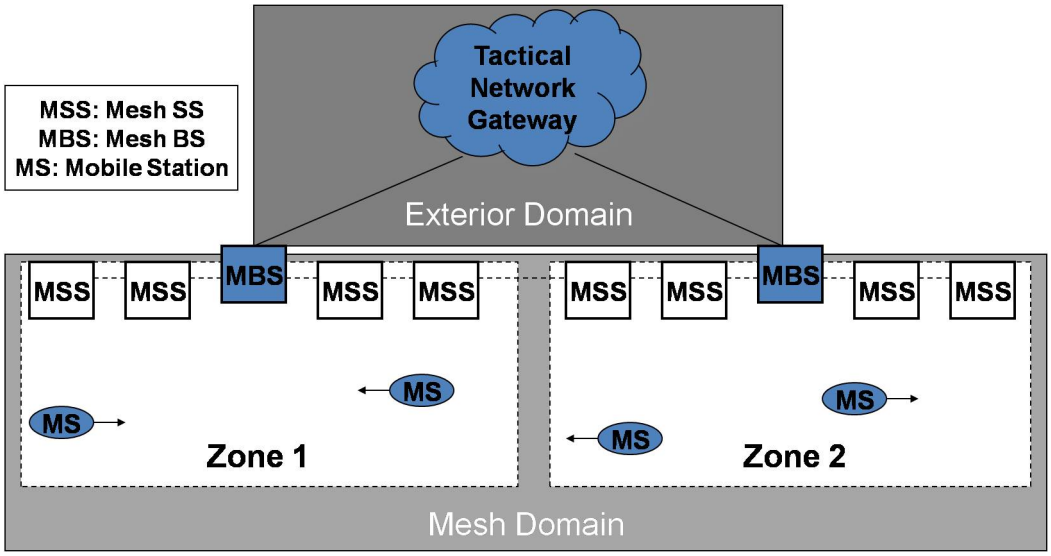

Figure 4.1: Routing Zone Structure

agent starts tunneling cached packets and new packets for the MS towards the care-of address. Optionally, the home agent may notify Mobile-IP-enabled senders to redirect their future packets to the care-of address directly. Assured of seamless mobility, the MS continues using its home address for sending and receiving IP packets via the foreign agent as its default gateway.

For the proposed network, Mobile IP is deployed by having each Mesh BS host the home agent and foreign agent services. Hence, a MS acquires its home address with the Mesh BS of the first connected intra-gateway routing zone. Then, it registers with a new foreign agent whenever entering a new routing zone. Re-association with a new foreign agent represents an opportunity of route optimization via a closest backhaul link, since it usually results in a shorter and more reliable route to the core network. The frequency of such re-association is determined by the choice of routing zone sizes. The signaling latency of such re-associations is masked by the MAIGR protocol and has minimal effects to the communication continuity. In the case of scarce backhaul bandwidth, the Mesh BS foreign agents can selectively bypass the

re-association procedure, and the MS communication will persist transparently.

Within each intra-gateway routing zone, each BS executes the MAIGR protocol to: 1) route packets from a MS towards the zones Mesh BS, and 2) route packets from a mesh or backhaul link towards a MS. The protocol maintains the following:

(1) Next hop towards closest Mesh BS:

Upon deployment and periodically, Mesh BSs send a flooding message with a forwarding hop count updated by all relaying Mesh SSs. The message ends at another Mesh BS or a specified maximum hop count. Each Mesh SS records the next hop towards the least hop-distance Mesh BS.

(2) Next hop towards a MS, at the serving BS:

At the current serving BS of an MS, the next hop is the active data connection of the MS, denoted with its connection identifier (CID). The routing table is updated during network entry and each handover.

(3) Next hop towards a MS, at a non-serving BS:

At any non-serving BS, the next hop is either a mesh link in the direction of the MS (denoted with the mesh connection's CID) or unknown. In non-trivial cases, the MS must be associated with another BS, which need not be in the same routing zone. A BS acquires knowledge of next hop towards the MS when the MS enters the network and/or when it hands over to a different BS by:

(i) when receiving from a neighboring BS a forwarded packet sent by an unknown MS, record the BS as next hop to the MS.

(ii) when notified of a handover of a currently associated MS, record the target BS as next hop to the MS.

(4) Next hop towards an exterior network:

For Mesh SSs, next hop towards an exterior network is always its Mesh BS. For Mesh BSs, next hop towards an exterior network is a pointer to its IP routing

agent.

Upon an MS's initial network entry, it sends out a DHCP request to the closest BS for acquiring its home address. The request is forwarded towards the Mesh BS (home agent) by potentially multiple Mesh SSs, who will all have learned the next hop towards the MS. Upon each handover, a handover indication message indicating the target BS is sent to the serving BS. The network layer is informed of the handover with the target BS address for updating the next hop to the MS. Note that the target BS can belong to a routing zone different from that of the serving BS. When an MS moves into a new routing zone, its incoming packets are delivered uninterrupted over the mesh from the previous routing zone. Until the time the new zones foreign agent establishes re-association with the home agent and starts receiving packets via the new zone's backhaul link, the packets continue to be delivered over the mesh and the transition is transparent to the MS. While it may potentially cause out-of-order arrivals from the mesh and backhaul links, it assures that no packets are dropped due to no route to the MS at any time.

Chapter 5

Scheduling Algorithm

The scheduling solution consists of two scheduling implementations: PMP mode scheduling and mesh mode Scheduling. The PMP mode scheduler is used to derive a contention-free data transmission schedule between a BS (MBS, MSS) and MSs. The mesh mode scheduler dervies a contention-free data transmission schedule between BSs that form the mesh backhaul. Each BS runs both PMP mode scheduler and a mesh mode scheduler, whereas each MS runs a PMP mode scheduler. At each BS, the PMP mode scheduler and mesh mode scheduler work in conjunction to adapt to the changes in traffic demands caused by the mobility of various MSs. Each scheduler transmits traffic in a structured OFDM frame format reviewed in Chapter 2.

5.1 PMP Mode Scheduling

The PMP mode scheduler is implemented at each BS independently. A BS divides the PMP frame into uplink and downlink sub-frames and further divides each subframe into mini-slots to be allocated to MS connection requests according to their

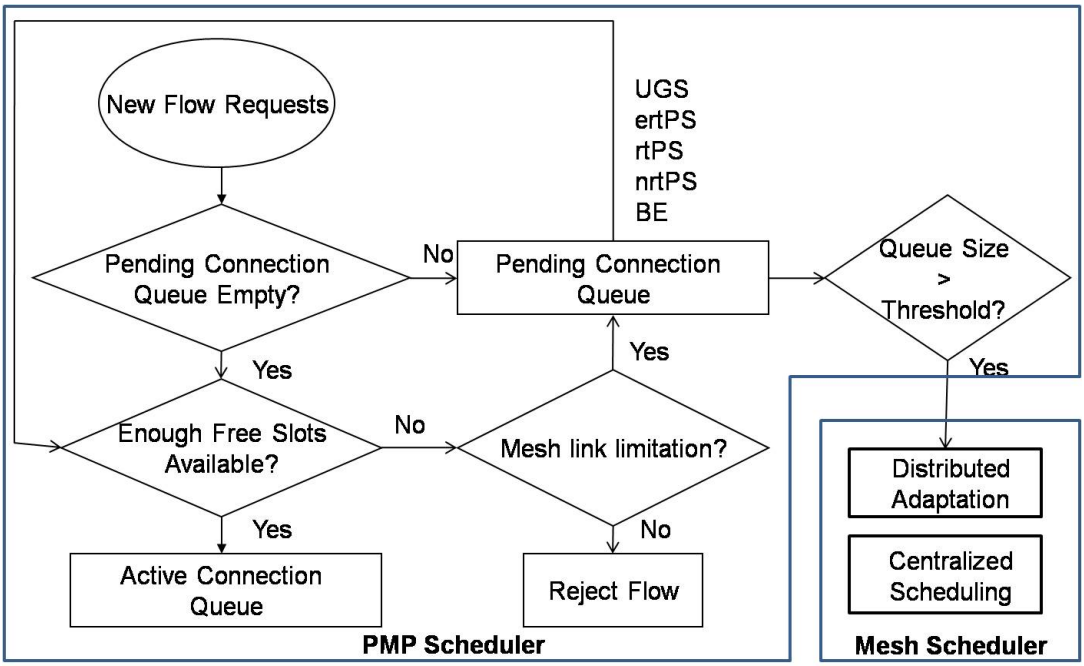

Figure 5.1: PMP Scheduler Flowchart

respective demand. The scheduler accounts for different service class priorities by allocating mini-slots to connection requests in the order of UGS, ertPS, rtPS, nrtPS and BE connections. All requests that are allocated their needed time are added to an active connection queue. The remaining unsatisfied requests will be handled according to the reason why the demand cannot be satisfied. An overview of the PMP mode scheduler can be seen in the flowchart represented in Figure 5.1.

Since all MS traffic must be relayed over the mesh links to reach a MBS, the available time a BS should allocate is limited by not only the PMP link capacity, but also the mesh link capacity. The BS will only accept requests up to the minimum of the two capacities. Thus, if a connection request cannot be satisfied due to exceeding the mesh link capacity but not the PMP capacity, the request is placed in a pending connection queue; only if the PMP capacity is exceeded, the request is rejected. Requests from the pending queue will be accepted according to the service class

priority order (UGS, ertPS, rtPS, nrtPS, BE) whenever currently occupied mini-slots become available. For two or more requests with the same service class priority, a First In First Out approach is used allowing the earlier arrived request to be serviced first. The pending queue also provides an indication of insufficient mesh link capacity, which can be dynamically adapted with the distributed schedule adaptation procedure described in Section 5.2.2.

5.2 Mesh Mode Scheduling

The mesh mode scheduler utilizes a centralized algorithm to determine the initial schedule and then a distributed adaptation procedure to cope with dynamic changes in the traffic loads. The centralized scheduler is incurred every time a new BS is added to the network. The distributed adaptation is incurred whenever the pending queue length exceeds a predefined threshold. The mesh mode scheduler concerns only mesh nodes, i.e., the MBSs and MSSs.

Figure 5.2 summarizes the scheduling algorithm parameters. Subscripts i and j are used to denote any two mesh nodes connected over their mesh interfaces. Each parameter is an estimate based on monitored long-term average traffic load at each BS. The algorithm assumes a network topology determined by the MAIGR protocol, where each MSS relays traffic to and from its closest MBS over the shortest path.

5.2.1 Centralized Scheduling

When a new MSS enters the mesh, it sends a network entry message (in the network control sub-frame) that is forwarded throughout the routing zone to inform the MBS and all MSSs in the zone. Each MSS then sends a message to the MBS (in the schedule control sub-frame) stating its uplink and downlink transmission

r_{ij}^{u} : Uplink data transmission rate
r_{ij}^{d} : Downlink data transmission rate

$b_i[s_i]^u$: Uplink PMP mode bandwidth demand (in bytes) for service type s_i
$b_i[s_i]^d$: Downlink PMP mode bandwidth demand (in bytes) for service type s_i

$d_i^u[s_i]$: Aggregate PMP mode uplink bandwidth demand (in bytes) for service type s_i
$d_i^u[s_i] = b_i[s_i]^u + \Sigma j \in child(i)\ b_j[s_i]^u$
where child(i) is any base-station j that has to forward its traffic to base-station i to reach MBS

$d_i^d[s_i]$: Aggregate PMP mode downlink bandwidth demand (in bytes) for service type s_i
$d_i^d[s_i] = b_i[s_i]^d + \Sigma j \in child(i)\ b_j[s_i]^d$
where child(i) is any base-station j that has to forward its traffic to base-station i to reach MSS

$T_i[s_i]^u$: Uplink PMP mode Transmission time demand for service type s_i
$T_i[s_i]^u = d_i[s_i]^u / r_{ij}^u$

$T_i[s_i]^d$: Downlink PMP mode Transmission time demand for service type s_i
$T_i[s_i]^d = d_i[s_i]^d / r_{ij}^d$

Figure 5.2: Mesh Scheduling Metrics

time demands, $Ti[Si]^u$ and $Ti[Si]^d$, respectively, for all service classes Si. All this transmission demand has to be accomodated in one mesh frame. So if the overall transmission demand is greater than the frame duration, the Mesh BS scales the transmission demand from each Mesh SS proportionally (using the number of routing-hops from itself to the Mesh SS) to fit the frame duration. Given all the transmission demands, the MBS executes the centralized scheduling algorithm as presented in Figure 5.3 to derive a new initial schedule. The schedule is sent to all MSSs in a scheduling message in the schedule control sub-frame. If the transmission demand at any MBS is not known, e.g. during network entry, a negative number is sent for traffic demand as an indicator. Uniform traffic distribution is assumed in such case to derive the new initial schedule. The copy of the initial schedule is stored at each MSS throughout network operation until a new initial schedule is generated when a new node enters or leaves the network.

```
t ← 1          // t represents one data mini-slot
For Each S_j   // j ∈ [1 (UGS), 2 (ertPS), 3 (rtPS), 4 (nrtPS), 5 (BE)]
    Y_i = T_i[S_j]/Mini-Slot Interval   // i ∈ [1, #BSs in a routing zone]
    While exists any Y_i > 0
        k ← arg max Y_i // Select the station with largest requirement
            i ∈ [1, #BSs in a routing zone]
        B ← ∅ // set of blocked links in this iteration
        A ← ∅ // set of active links in this iteration
        While k ≠ ∅
            Add k to A
            Add Blocked_Neighbor(k) to B
            k ← arg max Y_i
                i ∈ [1,#BSs in  a routing zone]; i ∉A ∪ B; Y_i > 0
        End while
        ActiveLinks(t) ← A
        t ← (t+1)
        Y_i ← Y_i− 1 for all i ∈ A
    End while
End For
```

Figure 5.3: Centralized Scheduling Algorithm

In the algorithm, mini-slot allocation of one mesh frame needs to be determined. The MBS estimates the uplink and downlink traffic ratio and divides the data sub-frame of the mesh frame into a proportionate number of uplink and downlink mini-slots. Scheduling is done on a slot-by-slot basis according to the traffic demand for various service classes. The order of service classes are determined with respect to class priority which follows the order: UGS, ertPS, rtPS, nrtPS and BE. Within each class, the transmitting node for the link which has the largest transmission demand is granted the first slot to transmit its traffic. Using the largest transmission demand criteria repetitively, non-interfering nodes are added incrementally to the list of active nodes for the same slot. Non-interfering nodes are based on concept of blocked neighbor. Each neighbor within transmission range of the transmitting MSS is considered to be a blocked neighbor. Once all possible active nodes for one slot are determined, the same procedure is followed for the successive mini-slots.

```
Maximum_Slots_to_Lend = Requested_Slots
If (Requesting_BS ∈ Routing_Child)
  Maximum_Slots_to_Lend = Min (Requested_Slots, (My_Current_Slots –
                                Active_PMP_Slots – Requesting_BSs_Current_Slots)/2)

Free_Slot_List ← ∅
For t ←1 to Slots_per_Frame          // t represents one data mini-slot
  If (t ∈ (Inactive _PMP_Slot) || (Unassigned_Slot))
    Add t to Free_Slot_List
End For
Send Maximum_Slots_to_Lend && Free_Slot_List
```

Figure 5.4: Distributed Adaptation Algorithm

5.2.2 Distributed Schedule Adaptation

Distributed scheduling messages are sent between 2-hop neighboring BSs in schedule control sub-frames to adapt the mesh link schedule to better suit the needs of current traffic-load. A three way handshake technique is used by the BS to determine if it can use any of the mini-slots currently assigned to its neighboring BSs. Each BS monitors its pending connection queue and computes additional required uplink and downlink transmission times in terms of mesh frame mini-slots. These additional required mini-slots and the currently assigned mini-slots are sent by the requesting BS to its 2-hop neighboring BSs. These neighbors respond to this request according to the algorithm described in Figure 5.4 by sending all mini-slots that it can offer to lend in one mesh frame and the upper bound on how many of these slots the requesting BS is allowed to use. Once the requesting BS receives the response from all of its 2-hop neighbors, it identifies maximum common mini-slots that are offered and sends an acknowledgment to all its 2-hop neighbors of using these slots.

Every MSS keeps track of the number of mini-slots it has been assigned per

mesh frame. This information is needed at each MSS which participates in the distributed adaptation procedure presented in Figure 5.4. When the borrowing request reaches an MSS (lender), it first sets the number of maximum mini-slots it could lend equal to mini-slots requested by the borrowing MSS. If the lending MSS is located closer to the MBS than the borrowing MSS, an amount equal to mini-slots that are offered to be lended have to be reserved by the lending MSS because all the traffic supported by the lended slots is going to traverse through the lending MSS on its way to the MBS. In this case, the maximum mini-slots the lending MSS can lend is the minimum of these two values: (a) requested mini-slots by the borrowing MSS and (b) mini-slots that remain at lending MSS after the reservation. On the other hand, if the lending MSS is located away from the MBS than the borrowing MSS, the lending MSS does not need to reserve any mini-slots since the traffic supported by the lended mini-slots is not going to traverse through the lending MSS on its way to the MBS. Once the number of maximum lendable mini-slots is determined, the lending MSS goes through all the mini-slots in one mesh frame and builds a list of mini-slots not being used (i.e. (a) the ones that are not assigned to it or (b) the ones that are assigned to it but are not being used). This list along with the number of maximum lendable mini-slots is sent to the borrower which uses this information to determine if it can use any of the offered mini-slots. Once the borrower determines the particular mini-slots it is borrowing, it sends this information to all MSSs that participated in the current lending process.

Chapter 6

Analytical Model and Simulation Studies

The proposed network architecture, scheduling and routing solution is ideal for vehicular and tactical military networks. For such networks, various common deployment topologies are viable alternatives. The performance of the proposed solution is analyzed for two deployment scenarios - chain topology and single intersection topology, and steps to obtain similar analytical model for grid topology is presented. In each topology, the network architecture divides the deployed base stations into separate routing zones. Analysis is performed for one routing zone. The number of base stations in a routing zone depends on the availability of backhaul-enabled base stations (MBSs). Each routing zone consists of exactly one MBS and several other base stations (MSSs) that forward traffic through MBS to reach the core network. In addition, each base station supports Mobile Stations (MSs) within its PMP mode communication range. So, the overall traffic experienced at each base station is an aggregate of its own PMP mode traffic and the mesh traffic forwarded by other base stations on its way to the MBS. Due to the traffic aggregation concept, the mesh links

closer to MBS are going to be more heavily loaded than the ones away from it. So, the placement of the MBS in the center of the routing zone is a logical deployment choice and MSSs should expand symmetrically on either side of the MBS.

The purpose of mesh scheduling solution is to allocate the data slots of one mesh frame to different mesh links. The number of data slots in one mesh frame depends on the modulation scheme used and is treated as a variable in this analysis. The mesh scheduling solution implements frequency reuse by allowing non-interfering nodes to transmit simultaneously as described by the centralized mesh scheduling algorithm in Chapter 5. To determine if a particular node would interfere with any other transmitting node, carrier sensing range metric of each node has to be considered. Carrier sensing range depends on receiver sensitivity and is used in context of number of hops in this analysis. Carrier sensing range is assumed to be always greater than or equal to the communication range. The communication range of each node is assumed to be equal to 1 in the analysis. MBSs and MSSs within the carrier sensing range of each other are considered as interfering nodes and may not transmit simultaneously. Table 6.1 summarizes all the relevant parameters considered in the analysis.

As noted earlier, the placement of the MBS in the center of the routing zone is a logical deployment choice due to traffic aggregation concept and MSSs should expand symmetrically on either side of the MBS. So, $n'=n$ for all representations of n' in Table 6.1. The values n and n' are presented separately in Table 6.1 because of the naming convention used to pictorially represent the network topology during the analysis. The value n and n' are interchangeable anywhere in the derivation of analysis that follows.

Parameter	*Chain Topology*	*Single Intersection Topology*	*Grid Topology*
Number of Mesh BS	1	1	1
Number of Mesh SS	n+n′	2(n+n′)	$n * n'$
Number of Mesh Links	n+n′	2(n+n′)	variable
PMP Traffic Load at Mesh SS k	X_k	X_k	X_k
Mesh Traffic Load for Link k	$\sum_{i=k}^{n} X_i$	$\sum_{i=k}^{n} X_i$	variable
Data slots per Mesh Frame	z	z	z
Carrier Sensing Range	y	y	y
Communication Range	1	1	1

Table 6.1: Analytical Model Relevant Parameters

6.1 Chain Topology

The chain topology corresponds to a typical vehicular network deployment along a single interstate highway. A symmetric chain topology containing the information about traffic load at each mesh link is shown in Figure 6.1. The figure also establishes the base station and mesh link number scheme to be used in the analysis.

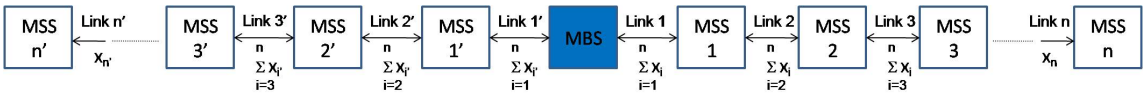

Figure 6.1: Chain Topology

Each base station runs an initial centralized algorithm to come up with mesh link schedule. Based on the mesh link schedule, a PMP mode schedule is generated by each base station independently to communicate with the mobile stations (MS). To be fair in terms of MS traffic supported at each base station, uniform traffic distribution is assumed during initial network deployment and this is the information used by

the centralized mesh scheduling algorithm to come up with an initial mesh schedule. Under this assumption,

$$PMP\ Traffic\ Load\ at\ Mesh\ SS\ k\ =\ X_k\ =\ x \tag{6.1}$$

$$Mesh\ Traffic\ Load\ at\ Link\ k\ = \sum_{i=k}^{n} X_i = (n-k+1)x. \tag{6.2}$$

The resulting mesh link demands can be seen in Figure 6.2.

Figure 6.2: Uniform Traffic Demand in Chain Topology

Unidirectional traffic is considered while scheduling mesh link traffic. So the traffic is either moving towards the Mesh BS or is moving away from the Mesh BS throughout the chain topology. Since Mesh BS is at the center of the chain, the traffic flow is symmetric with respect to the Mesh BS. Referring to the numbering scheme used in Figure 6.1, all Links k where k $\in [1, n]$ will have traffic flow in the same direction. This direction is opposite to the traffic flow direction for all Links k′ where k′ $\in [1', n']$. An example of traffic flow direction is given in Figure 6.3 with n = n′ = 4.

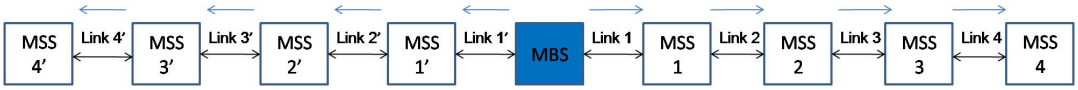

Figure 6.3: Traffic Flow Direction

The carrier sensing range metric, y, determines the minimum spacing between two mesh links that can transmit simultaneously. Define minimum spacing as the

number of links that are required to be inactive between two closest active links. For two active links with the same traffic flow direction, the minimum spacing is y+1. For two active links with opposite traffic flow direction, the minimum spacing is y. As an example, consider Link 1 in Figure 6.3 and let y = 1. If Link 1 is active, for the same direction traffic flow links (Links 2, 3 and 4), minimum spacing is y+1=2 and so Link 4 is the closest possible active link. For the opposite direction traffic flow links (Links 1′,2′,3′ and 4′), minimum spacing is y=1 and so Link 2′ can be the closest possible active link.

Since the centralized scheduling algorithm selects the active links in order of highest transmission demands, the most heavily loaded links are going to be allowed to transmit first by the scheduler. This follows the order: 1,1′, 2,2′, 3,3′, 4,4′.....n,n′. The lighter traffic demand links transmit simultaneously with heavily loaded links depending on minimum spacing requirement. So to analyze the performance of one routing zone, the goal is to identify the heavily loaded links that cannot transmit simultaneously and then consider links that do not meet minimum spacing requirement when these heavily loaded links are active. Starting from heaviest loaded links, Link 1 and 1′, and using symmetry, the traffic demand for links that cannot simultaneously transmit are given by L represented in Equation 6.3 and 6.4 for odd and even carrier sensing range values respectively.

For odd carrier sensing range value,

$$L = 2 * \sum_{i=1}^{\lceil y/2 \rceil} Mesh\ Traffic\ Load\ at\ Link\ i \tag{6.3}$$

For even carrier sensing range value,

$$L = 2*(\sum_{i=1}^{y/2} Mesh\ Traffic\ Load\ at\ Link\ i) + Mesh\ Traffic\ Load\ at\ Link\ (y/2+1) \tag{6.4}$$

Now that the traffic demand for the heaviest loaded links that cannot transmit simultaneously is identified, links that do not meet minimum spacing requirement when these links are active have to be considered. Since the more stringent minimum spacing requirement is y+1 links for same direction traffic flow, only y+2 links in each direction (because of symmetry) have to considered in the analysis. L includes all the links that cannot simultaneously transmit. So, the links that are still unaccounted for are represented by the following range: Links $[1, y+2] \notin L$. The traffic demands at these links have to be checked for simultaneous transmissions with the links accounted for by L. The unsatisfied traffic demand due to the lack of simultaneous transmission capabiltiy from these links can be represented by L^* given in Equation 6.5 and 6.6 for odd and even carrier sensing range values respectively.

For odd carrier sensing range value,

$$L^* = \sum_{i=\lceil y/2 \rceil+1}^{y+2} Mesh\ Traffic\ Load\ at\ Link\ i\ - \sum_{i=1}^{\lceil y/2 \rceil} Mesh\ Traffic\ Load\ at\ Link\ i \tag{6.5}$$

$If L^* \leq 0, L^* = 0.$

For even carrier sensing range value,

$$L^* = \sum_{i=y/2+1}^{y+2} Mesh\ Traffic\ Load\ at\ Link\ i\ - \sum_{i=1}^{y/2} Mesh\ Traffic\ Load\ at\ Link\ i \tag{6.6}$$

$If L^* \leq 0, L^* = 0.$

The total transmission demand that needs to be satisfied per mesh frame can

be represented by T given in Equation 6.7.

$$T = L + L^* \tag{6.7}$$

T can be represented in terms of x, the PMP traffic load at Each Mesh SS k where $k \in [1, n]$ using Equations 6.2-6.7. Once T is represented in terms of x, T can be set equal to z, data slots per Mesh Frame and the value of x can be obtained in terms of slots per Mesh Frame. In turn, the value of x in terms of slots per Mesh frame can be used to represent PMP mode traffic supported by each base station. The PMP mode scheduler utilizes this information to generate the PMP mode schedule. So, x is the supported traffic in terms of slots per Mesh Frame at each base station according to the initial centralized mesh schedule. The actual demands may vary according to the distribution of MSs at each base station at any given point. If x is not sufficient to support required MS traffic, a distributed adaptation is used by the base stations which allows any base station to borrow data slots from neighboring base stations. Two extreme cases for the distributed adaptation are considered, dense network where borrowing opportunities are limited or almost non-existent, and sparse network where borrowing can occur freely and analysis is performed for both cases.

6.1.1 Dense Network

A dense network represents every base station (MBS and MSS) having enough subscriber stations (MSs) to operate at full PMP mode capacity. An example dense network topology is presented in Figure 6.4. Using this topology, the limitation on how much traffic can be supported at each base station is going to be bound by the mesh link capacity which is computed by the centralized mesh scheduling algorithm. Due to the nature of service classes supported by WiMAX standard, there are cases

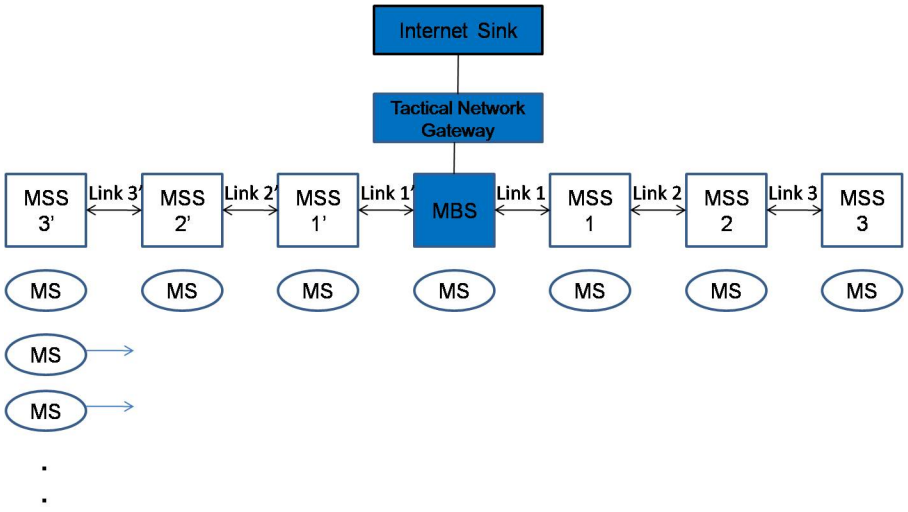

Figure 6.4: Dense Network Topology

where all the allocated mesh slots might not be perfectly used up by every base station. So, there are two cases for which analysis using the distributed adaptation is possible:

1) If all the allocated slots, x, computed by initial centralized mesh algorithm are used up perfectly at each base station, then there are no slots at any neighboring base stations that can be borrowed. In such case, the distributed adaptation is not going to be helpful and the overall network throughput observed when using centralized algorithm without the distributed adaptation is going to be the same as when the distributed adaptation is used. So, there is no gain in overall network throughput.

2) If all the allocated slots, x, computed by initial centralized mesh algorithm are not perfectly used up at each base station, then there might be a possibility for some of the base stations to borrow slots from neighboring base stations. In such case, the distributed adaptation is going to improve the overall network throughput slightly over a centralized only approach. For analysis purposes, let q_i represent

the number of assigned slots in the mesh frame not being used by base station i. Subscript k represents MSS that is borrowing, and subscript j represents MSS that is lending data slots. The improvement in overall network throughput is upper bound by Equation 6.8 if the borrowing MSS borrows slots from another MSS located farther from the MBS and by Equation 6.9 if the borrowing MSS borrows slots from another MSS located closer to the MBS.

$$\%\ increase(\gamma) = (((2 * q_j) + q_k)/(z - \sum_{i=1}^{n+n'} q_i)) * \ 100\ where\ z\ >>\ q_i\ for\ all\ i \quad (6.8)$$

$$\%\ increase(\gamma) = (((q_j/2) + q_k)/(z - \sum_{i=1}^{n+n'} q_i)) \ * \ 100\ where\ z\ >>\ q_i\ for\ all\ i \quad (6.9)$$

All q_i terms are going to be small compared to z, data slots per mesh frame. So the increase in overall network throughput should be very small. Simulation results presented in section 6.1.3 verifies that the increase in overall network throughput is minimal.

6.1.2 Sparse Network

A sparse network represents very lightly loaded network. In such topology, all MSs may be concentrated at one base station as seen by an example sparse topology represented by Figure 6.5. So there are plenty of borrowing opportunities available since all the mesh slots assigned to every base station by the initial centralized mesh scheduling algorithm are not going to be used up. Again, due to the nature of service classes supported by WiMAX standard, there are cases where all the allocated mesh

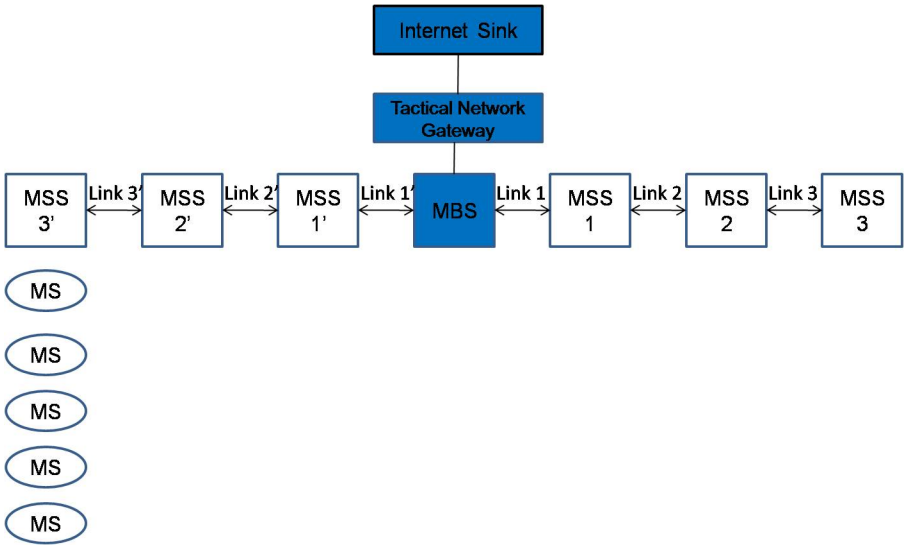

Figure 6.5: Sparse Network Topology

slots might not be perfectly used up by every base station. So, there are two cases for which analysis using the distributed adaptation is possible:

1) If all the allocated slots, x, computed by initial centralized mesh algorithm are used up perfectly at each base station, then there are no currently unused slots at any base stations that can be used once additional borrowed slots are gained. As a result, the distributed adaptation is going to improve the network performance by utilizing borrowed slots only. In such case, the improvement in overall network throughput is upper bound by Equation 6.10 if the borrowing MSS borrows slots from another MSS located farther from MBS and by Equation 6.11 if the borrowing MSS borrows slots from another MSS located closer to the MBS.

$$\% \; increase(\gamma) = 2 \; * \; 100 = 200\% \tag{6.10}$$

$$\% \; increase(\gamma) = (1/2) \; * \; 100 = 50\% \tag{6.11}$$

where n = number of Mesh SS and $k \in [1, n]$

2) If all the allocated slots, x, computed by initial centralized mesh algorithm are not perfectly used up at each base station, then there might be a possibility for some of the base stations to use the currently unused slots once it borrows additional slots from neighboring base stations. Under these circumstances, the improvement in overall network throughput using the distributed adaptation is going to be greater than the improvement represented by Equations 6.10 and 6.11. In such case, the improvement in overall network throughput is upper bound by Equation 6.12 if the borrowing MSS borrows slots from another MSS located farther from the MBS and by Equation 6.13 if the borrowing MSS borrows slots from another MSS located closer to the MBS.

$$\% \; increase(\gamma) = ((2x + q_k)/(x - q_k)) \; * \; 100 \tag{6.12}$$

$$\% \; increase(\gamma) = (((1/2)x + q_k)/(x - q_k)) \; * \; 100 \tag{6.13}$$

where q_k represents currently unused slots at base station k.

6.1.3 Simulation Studies

A chain topology is simulated in ns-2 to assess the correctness of the analytical model. The simulated topology is presented in Figure 6.6 and the relevant parameters are listed in Table 6.2. An overview on some of the simulation implementation is presented in the simulator setup section in Appendix A.

Based on the parameters used in the simulation, the initial centralized mesh scheduling algorithm computes mesh data slot distribution presented in Table 6.3.

Figure 6.6: Mesh Simulation Topology

Parameter	***Value***
Number of Mesh BS	1
Number of Mesh SS	$3+3=6$
Number of Mesh Links	$3+3=6$
PMP Traffic Load at Mesh SS	x
Mesh Traffic Load for Link k	$\sum_{i=k}^{3} x = (3-k+1)x$
Data slots per Mesh Frame	172
Carrier Sensing Range	1
Communication Range	1

Table 6.2: Simulation Parameters

Setting T (total transmission demand per mesh frame) equal to z (data slots per mesh frame), i.e. $6x = 172$, x is obtained to be 28. So every MSS (MSS 1' - MSS 3', MSS 1 - MSS 3) in the simulation is assigned 28 data slots per mesh frame. This represents the amount of PMP traffic each MSS can support initially. Note that the supported traffic at MBS is not limited by mesh links. MBS can support bounded by its point-to-point backhaul link to the core network. Since the mesh link allocation at Link k is represented by $\sum_{i=k}^{3} x = (3-k+1)x$, Links 1, 2, and 3 have an allocation of 84, 56 and 28 respectively. Since the topology is symmetric, Links $1'$, $2'$ and $3'$ have the same distribution as Links 1, 2, and 3 respectively. Dense and sparse networks are studied for the chain topology and the improvement using the distributed adaptation over centralized scheduling is observed. Analytical model is verified using the simulation results.

Dense network topology is represented by having MSs at each base-station (MSS 1' - MSS 3', MBS, MSS 1 - MSS 3) as represented by Figure 6.4. To simulate

Parameter	***Value***
L	$2 * 3x$
L^*	0
T	$6x$
x	28

Table 6.3: Centralized Mesh Scheduling Parameters

heavy loads efficiently, packet sizes are selected to be 800 Bytes and so one data packet transmission takes up $/\lceil(800 * 8/856)\rceil = 8$ data slots. Each MS generates 2 flows of 0.64 Mbps UGS connections. Each flow generates $(0.64 * 10^6/8)$ Bytes/Sec * 0.010 Sec/Frame Duration = 800 Bytes/Frame Duration. Since 800 Bytes take up 8 data slots for transmission, each MSS can support a maximum of 3 flows of 0.64 Mbps UGS connections according to the initially generated centralized schedule. Five MS group sizes are studied. The first group size contains one MS at MSS $3'$ and one additional MS at every other MSS (MSS $1'$ - MSS $2'$, MSS 1 - MSS 3). The second group size contains two grouped MSs at MSS $3'$ and one additional MS at every other MSS. The third group size contains three grouped MSs at MSS $1'$ and one additional MS at every other MSS and the pattern follows. In the simulated scenarios, the grouped MSs are either static or moving from left to right. Results for both static and moving case are presented when only centralized mesh scheduling algorithm is used in Figures 6.7 and 6.8 respectively in terms of maximum overall throughput and number of pending flows.

For the static scenario, the overall observed throughput remains steady at around 8.27 Mbps. The maximum number of flows each MSS can support is 3. So once a group of 2 MSs is created, the total number of flows for the BS where the group is located reaches 4. Thus, one of the flows has to be put in the pending queue by the MSS. Following the same pattern, once more nodes accumulate at one MSS,

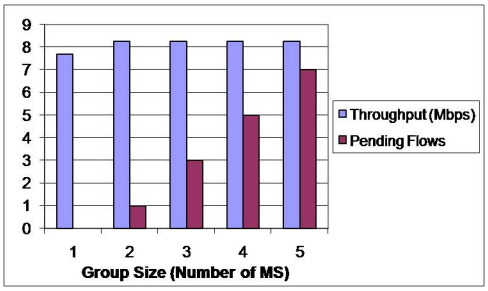

Figure 6.7: Static MS using Centralized Scheduling only

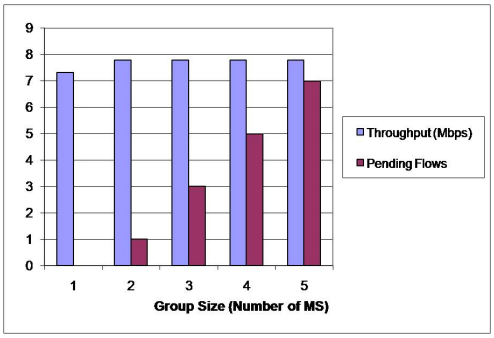

Figure 6.8: Moving MS using Centralized Scheduling only

the ensuing flows have to be put in the pending queue as well. The total number of maximum flows supported is 6*3=18 if the MSs are distributed such that 3 flows are created at each MSS. But in the simulated scenario, since 2 flows are created at each MSS except for the one where the group is located which can support a maximum of 3 flows, a total of (2*5)+3 = 13 flows can be supported. The moving scenario using the centralized scheduling also produces similar results as the static scenario as observed in Figure 6.8. The only difference is that the overall observed throughput is steady at around 7.79 Mbps instead of 8.27 Mbps. This is due to the effect of handovers during which some of the data slots are used for handover messages. So the movement of MS does not really affect the network performance critically.

In the dense network topology, using the distributed adaptation improves the

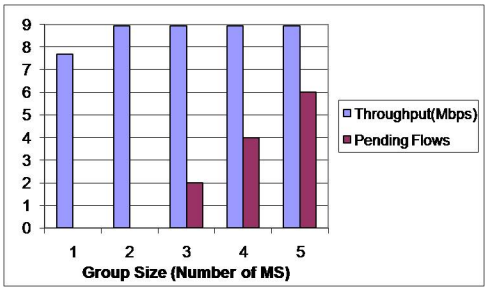

Figure 6.9: Static MS using Distributed Adaptation

overall performance slightly. Since the network is almost saturated, each MSS is supporting as many MSs as it could close to its PMP link capacity. There are not many data slots available for neighboring BSs to borrow when the network is dense. Data slots are borrowed by the BS where the grouped MSs are present and the capacity of the corresponding BS is increased from 3 UGS flows to 4 UGS flows. Thus, for group sizes of 1 and 2, there are no pending flows as can be observed in Figure 6.9. But once the group size increases to 3, 6 UGS flows are requested at one of the MSSs and the MSS cannot borrow any additional data slots from its 2-hop neighboring MSSs. Thus, 2 of the flows are kept in the pending queue and subsequent addition of flows experience the same fate. The overall network throughput stays steady around 8.95 Mbps. This results in an increase of 8.2% (from 8.27 Mbps to 8.95 Mbps). This result approaches the theoretical upper bound which is 9.6% as calculated in Equation 6.14. Thus, throughput performance using distributed adaptation is very similar to the centralized only approach for dense networks.

Referring to Equation 6.9,

$$q_i = 28 - (8 * 3) = 4 \; for \; MSS \; where \; a \; group \; of \; MS \; is \; located$$

$$q_i = 28 - (8 * 2) = 12 \; for \; every \; other \; MSS \; i$$

$$z = 168$$

$$\%\, increase(\gamma) = ((4+(12/2))/(168-(4+12+12+12+12+12)))* 100 \;=\; 9.6\% \quad (6.14)$$

The upperbound on the percentage increase in network throughput is 9.6 %. The observed increase is 8.2 %. The upperbound is achieved if all the data slots after borrowing are used up. In the simulated case, this does not happen. MSS $3'$ borrows $4 + (12/2) = 10$ slots. It can only use 8 of those slots to add one addtional flow. So 2 of the borrowed slots are not used. As a result, the increase is $8/104 \approx 8.0\%$ instead of $10/104 = 9.6\%$.

Sparse network load offers MSSs greater flexibility in terms of borrowing data slots from its neighbors. An extreme case is simulated where all MSs gather at one MSS as depicted in Figure 6.5 earlier. All other MSSs have no PMP traffic to support. In such case, the overall network throughput supported increases drastically when using the adaptive distributed approach as compared to only centralized approach as depicted in Figure 6.10. If 10 MSs each requesting one 0.64 Mbps UGS flow are all located at MSS $2'$, the increase in overall network throughput is about 232 % (from 1.92 Mbps to 6.38 Mbps). This refers to the case where borrowing occurs from an MSS located away from MBS. If 5 MSs each requesting one 0.64 Mbps UGS flow are all located at MSS $1'$, the increase in overall network throughput is about 66% (from 1.92 Mbps to 3.19 Mbps). This refers to the case where borrowing occurs from an MSS located closer to MBS. Both these cases satisfy the upperbound equations, Equations 6.12 and 6.13, which were obtained through analysis. The upperbound for this simulation scenario is expressed through Equations 6.15 and 6.16 respectively. An explanation on the observed results is given next.

$q_i = 28 - (8 * 3) = 4\ for\ MSS\ where\ traffic\ is\ located$

$$x = 28$$

Referring to Equation 6.12,

$$\%\ increase(\gamma) = (((2 * 28) + 4))/(28 - 4) * \ 100 \ = \ 250\% \tag{6.15}$$

Referring to Equation 6.13,

$$\%\ increase(\gamma) = (((1/2) * 28) + 4)/(28 - 4) * \ 100 \ = \ 75\% \tag{6.16}$$

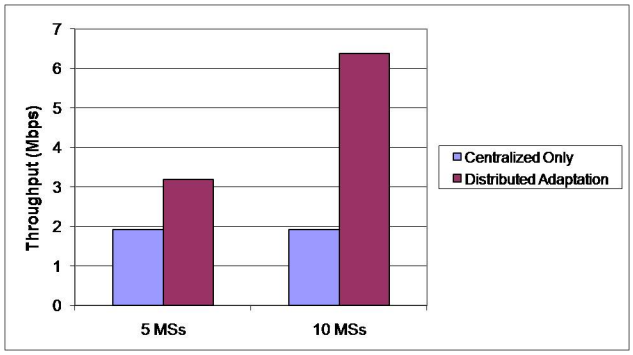

Figure 6.10: Static MS Throughput comparison for Sparse Network Scenario

The upperbound on the percentage increase in network throughput for scenario with 5 MSs is 75 %. The observed increase is 66 %. The upperbound is achieved if all the data slots after borrowing are used up. In the simulated case, this does not happen. Originally, 3 flows are supported at MSS 1′ which take up 24 slots. 28 slots are assigned to MSS 1′ by initial centralized scheduling algorithm. So, 28-24=4 slots are not being used. After the borrowing occurs, MSS 1′ has 28+14=42 slots. 5 flows can be supported using 40 slots since each flow takes up 8 slots. So, 2 slots are still not being used. If they would have been used up, then the increase in network throughput would have been $(42-24)/24*100\% = 75\%$. But since this is not the case, the increase

in network throughput that is observed is $(40-24)/24*100\% = 66\%$. The upperbound on the percentage increase in network throughput for scenario with 10 MSs is 250 %. The observed increase is 232 %. Again, the upperbound is achieved if all the data slots after borrowing are used up which does not happen in the simulated case. Originally, 3 flows are supported at MSS $2'$ which take up 24 of the 28 slots assigned by initial centralized scheduling algorithm. So, 28-4=4 slots are not being used. After the borrowing occurs, MSS $2'$ has 28+56=84 slots. 8 slots can be supported using 80 slots. So, 4 slots are not going to be used. Thus, the increase in network throughput is $(80 - 24)/24 * 100\% = 232\%$ instead of maximum possible increase which is $(84 - 24)/24 * 100\% = 250\%$.

6.2 Single Intersection Topology

The single intersection topology corresponds to a typical vehicular network deployment along two intersecting highways. A symmetric single intersection topology containing the information about traffic load at each mesh link is presented in Figure 6.11. Base station and mesh link number scheme used in the analysis is shown in the figure.

Each base station runs an initial centralized algorithm to come up with mesh link schedule. Based on the mesh link schedule, a PMP mode schedule is generated by each base station independently to communicate with the mobile stations (MS). To be fair in terms of MS traffic supported at each base station, uniform traffic distribution is assumed during initial network deployment. Under this assumption,

$$PMP\ Traffic\ Load\ at\ Mesh\ SS\ k\ =\ X_k\ =\ x \tag{6.17}$$

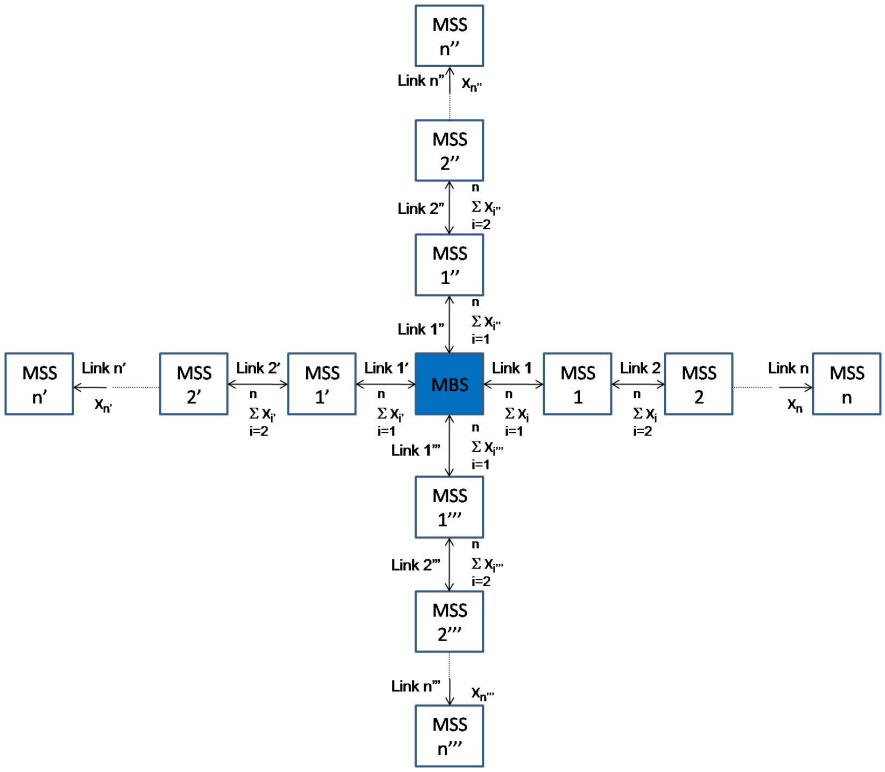

Figure 6.11: Single Intersection Topology

$$Mesh\ Traffic\ Load\ at\ Link\ k\ = \sum_{i=k}^{n} X_i = (n-k+1)x \tag{6.18}$$

The resulting mesh link demands can be seen in Figure 6.12.

Unidirectional traffic is considered while scheduling mesh link traffic. So the traffic is either moving towards the Mesh BS or is moving away from the Mesh BS throughout the single intersection topology. Since Mesh BS is at the center of the chain, the traffic flow is symmetric with respect to the Mesh BS. Referring to the numbering scheme used in Figure 6.11, all Links k where k $\in [1, n]$ will have traffic flow in the same direction. This direction is opposite to the traffic flow direction for all Links k′ where k′ $\in [1', n']$. Traffic flow direction for all Links k″ where k″ $\in [1'', n'']$ is 90° apart from the traffic flow direction of Links $[1, n]$. Traffic flow direction for all

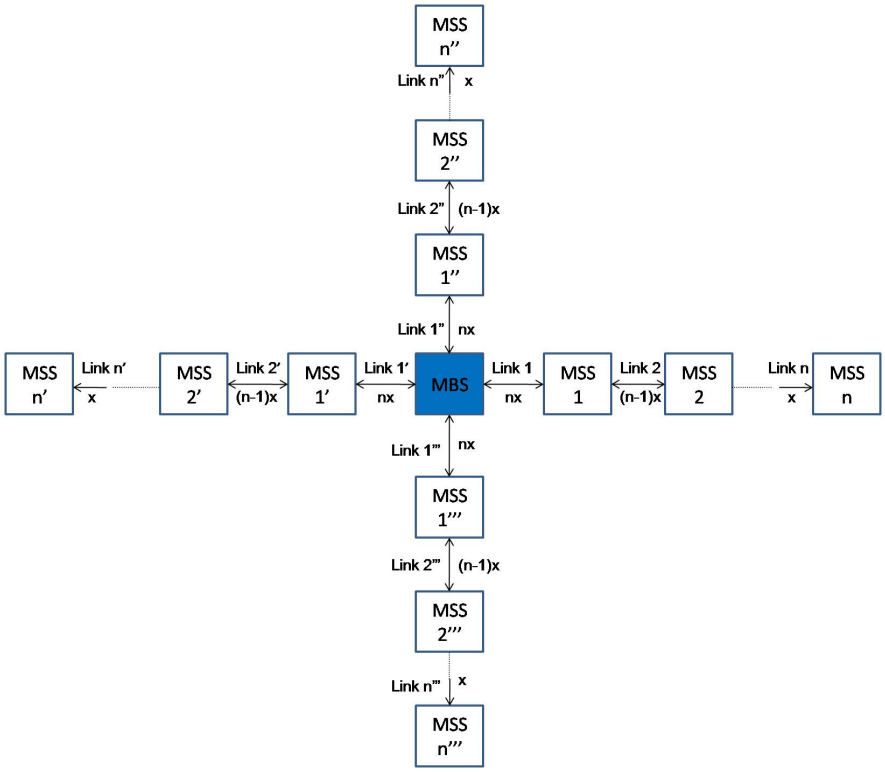

Figure 6.12: Uniform Traffic Demand in Single Intersection Topology

links k‴ where k‴ $\in [1''', n''']$ is exactly opposite to the traffic flow direction for all Links k″. An example of traffic flow direction is given in Figure 6.13 with n = n′ = n″ = n‴ = 3.

The carrier sensing range metric, y, determines the minimum spacing between two mesh links that can transmit simultaneously. As defined earlier in the Chain Topology section, minimum spacing refers to the number of links that are required to be inactive between two closest active links. For two active links with the same traffic flow direction, the minimum spacing is y+1. For two active links with any other (offset by 90° , 180° , or 270°) traffic flow direction, the minimum spacing is y. As an example, consider Link 1 in Figure 6.13 and let y = 1. If Link 1 is active,

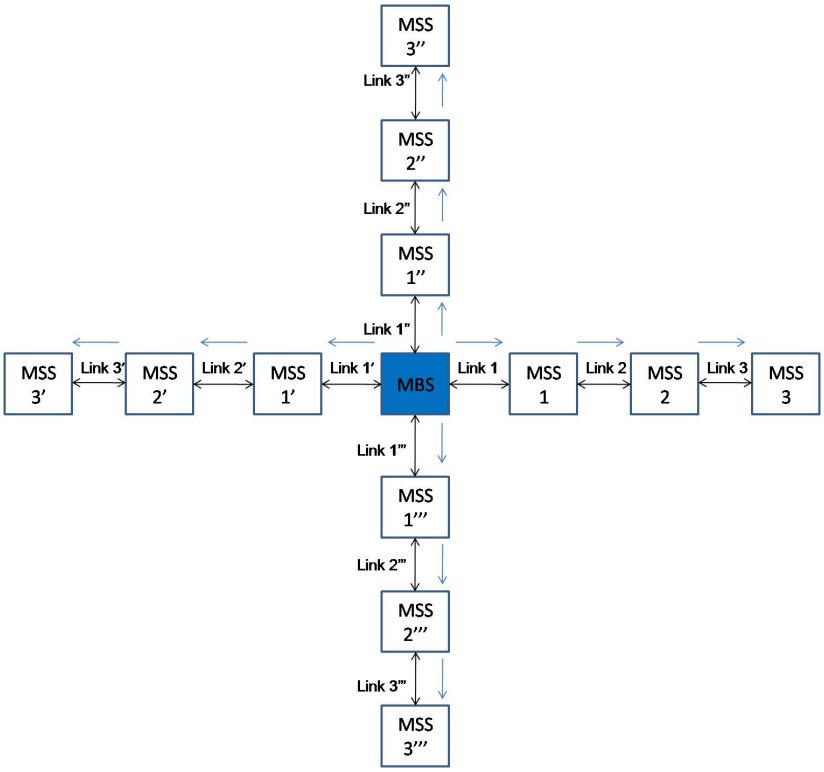

Figure 6.13: Traffic Flow Direction for Single Intersection Topology

for the same direction traffic flow links (Links 2 and 3), minimum spacing is y+1=2 and so none of the two links can be active. For the links with any other traffic flow direction, (Links 1′-3′, 1″-3″, 1‴-3‴), minimum spacing is y=1 and so Links 2′, 2″ and 2‴ can be the closest possible active links.

Since the centralized scheduling algorithm selects the active links in order of highest transmission demands, the most heavily loaded links are going to be allowed to transmit first by the scheduler. This follows the order: 1,1′,1″,1‴, 2,2′,2″,2‴, 3,3′,3″,3‴,.....4,4′,4″,4‴. While the heavily loaded links are allowed to transmit, the links with lighter traffic demands can simultaneously transmit depending on the minimum spacing requirement. When all the traffic demand for a heavily loaded link is satisfied, the lightly loaded link demand is automatically satisfied that meets the

minimum spacing requirement. So for analysis purposes, the goal again is to identify the heavily loaded links that cannot transmit simultaneously and then consider links that do not meet minimum spacing requirement when these heavily loaded links are active. Starting from heaviest loaded links, Link 1, $1'$, $1''$, $1'''$, and using symmetry, the traffic demand for links that cannot simultaneously transmit are given by L represented in Equation 6.19 and 6.20 for odd and even carrier sensing range values respectively.

For odd carrier sensing range value,

$$L = 4 * \sum_{i=1}^{\lceil y/2 \rceil} Mesh\ Traffic\ Load\ at\ Link\ i \tag{6.19}$$

For even carrier sensing range value,

$$L = 4*(\sum_{i=1}^{y/2} Mesh\ Traffic\ Load\ at\ Link\ i) + Mesh\ Traffic\ Load\ at\ Link\ (y/2+1) \tag{6.20}$$

Now that the traffic demand for the heaviest loaded links that cannot transmit simultaneously is identified, links that do not meet minimum spacing requirement when these links are active have to be considered. Since the more stringent minimum spacing requirement is y+1 links for same direction traffic flow, only y+2 links in each direction (because of symmetry) have to considered in the analysis. L includes all the links that cannot simultaneously transmit. So, the links that are still unaccounted for are represented by the following range: Links $[1, y+2] \notin L$. The traffic demands at these links have to be checked for simultaneous transmissions with the links accounted for by L. Since there are 3 traffic flow directions that are some offset of one of the traffic flow directions, the sum of the unsatisfied traffic demand has to divided by 3. The unsatisfied traffic demand due to the lack of simultaneous transmission capabiltiy

from these links can be represented by L^* given in Equation 6.21 and 6.22 for odd and even carrier sensing range values respectively.

For odd carrier sensing range value,

$$L^* = (\sum_{i=\lceil y/2 \rceil+1}^{y+2} Mesh\,Traffic\,Load\,at\,Link\,i)/3 - \sum_{i=1}^{\lceil y/2 \rceil} Mesh\,Traffic\,Load\,at\,Link\,i \tag{6.21}$$

$If L^* \leq 0, L^* = 0.$

For even carrier sensing range value,

$$L^* = (\sum_{i=y/2+1}^{y+2} Mesh\,Traffic\,Load\,at\,Link\,i)/3 - \sum_{i=1}^{y/2} Mesh\,Traffic\,Load\,at\,Link\,i \tag{6.22}$$

$If L^* \leq 0, L^* = 0.$

The total transmission demand that needs to be satisfied per mesh frame can be represented by T given in Equation 6.23.

$$T = L + L^* \tag{6.23}$$

T can be represented in terms of x, the PMP traffic load at Each Mesh SS k where $k \in [1, n]$ using Equations 6.18-6.23. Once T is represented in terms of x, T can be set equal to z, data slots per Mesh Frame and the value of x can be obtained in terms of slots per Mesh Frame. In turn, the value of x in terms of slots per Mesh frame can be used to represent PMP mode traffic supported by each base station. The PMP mode scheduler utilizes this information to generate the PMP mode schedule. So, x is the supported traffic in terms of slots per Mesh Frame at each base station according to the initial centralized mesh schedule. The actual demands may vary according to the distribution of MSs at each base station at any given point. If x is not sufficient

to support required MS traffic, a distributed adaptation is used by the base stations which allows any base station to borrow data slots from neighboring base stations.

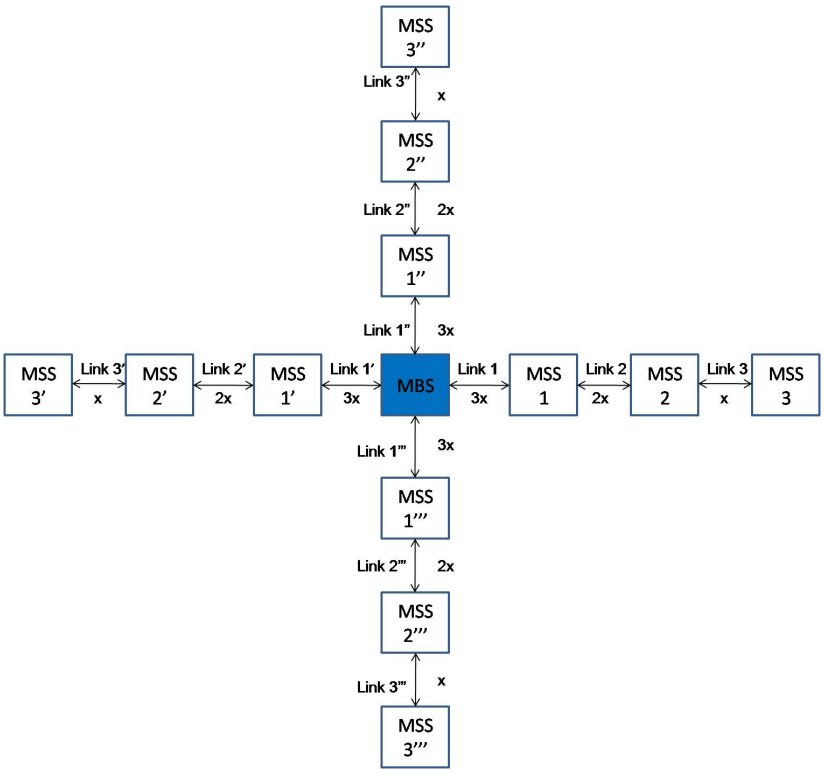

Figure 6.14: Single Intersection Simulation Topology

The analysis on using centralized algorithm only as compared to the distributed adaptation as well for both dense and sparse networks for the chain topology holds for the single interesection topology as well. So Equations 6.8 through 6.12 remain the same for single intersection topology. Simulations were run in ns-2 for topology presented in Figure 6.14 and same results were obtained as far as increase in overall throughput is concerned. The only difference was that x, the PMP traffic load supported at Each Mesh SS k was reduced by a factor of 2. So, for sparse scenario, when all MSs gather at one base station, the overall network throughput was reduced in half for both centralized only and distributed adaptation approach. But

the percentage increase remained the same when using distributed adaptation compared to centralized only approach as determined in the chain topology simulation results. For dense scenario, the overall network throughput results were identical to the chain topology simulation results.

6.3 Grid Topology

The grid topology corresponds to a typical metropolitan area network (MAN) deployment. An example two-dimensional symmetric grid topology with n=n′=5 is presented in Figure 6.15.

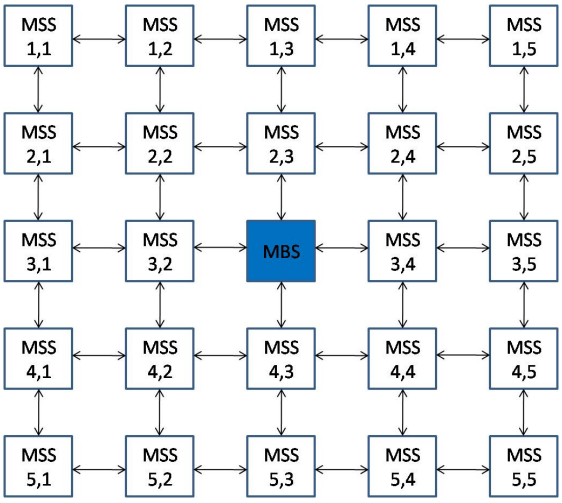

Figure 6.15: Grid Topology

In each routing zone, some MSSs have multiple routes that satisfy the minimum-hop criteria. For example, referring to the topology presented in Figure 6.15, MSS (2,2) can reach the MBS in 2 hops either using MSS (2,3) or MSS (3,2). Depending on the route chosen, the traffic demand at each mesh link would vary since the demand at each mesh link is an aggregate of the corresponding MSSs PMP mode traffic and all the traffic forwarded by other MSSs on its way to the MBS. As a result, the

initial centralized mesh scheduling algorithm would come up with a different data slot distribution for different routes chosen. Performance analysis depends on this initial distribution and hence different chosen routes would lead to a different set of equations for the performance analysis.

One of the ways the routes can be chosen would lead to a symmetric initial distribution. This would involve drawing two diagonals through the proposed topology and have each base station in four created partitions route through the MSSs only using other MSSs in the same partition. This phenomenon is illustrated as an example in Figure 6.16.

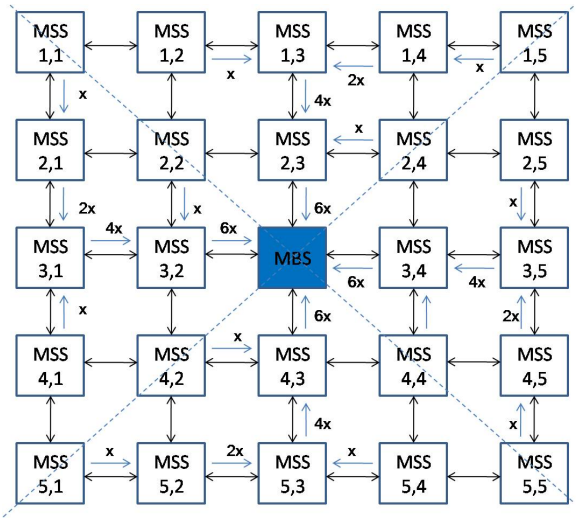

Figure 6.16: Grid Topology Symmetric Traffic Distribution

Analysis for the grid topology has not been performed yet and remains a topic of future work. The next steps for the analysis would be to come up with following:

1) Determine L and L^* as defined in Chain Topology and Single Intersection Topology. Due to the possibility of having a maximum of 4 1-hop neighbors, the carrier sensing range value is going to affect transmissions from separate partitions. Also, when considering the MSSs for minimum spacing, the flow direction in separate

partitions does not follow any pattern. This makes the calculation of L and L^* too complex to solve numerically. Computer aided simulation would be required to come up with these values.

2) Determine x, the PMP traffic load supported at each MSS. The procedure for calculating x remains the same. L + L^* represented in terms of x should be set equal to z and x should be solved for in terms of the number of data slots per mesh frame.

3) Once the initial mesh schedule has been determined using x, analysis for using centralized scheduling only versus distributed adaptation can then be performed for both dense and sparse networks using similar approach as presented in the Chain Topology section.

Chapter 7

Conclusions and Future Work

7.1 Conclusions

This thesis proposed an integrated routing and distributed scheduling approach for fast deployable IEEE 802.16e network where distributed base stations with dual radios form a mesh backhaul and subscriber stations communicate through these base-stations. The proposed routing protocol exploits the coverage continuity of the wireless mesh infrastructure to enhance communication persistence. Within the mesh, end-to-end routes between an MS and the core network adapt according to the movement pattern of the MS. Once reaching the backhaul-enabled BSs, packets are routed with globally addressed routing protocols such as Mobile IP or ad hoc routing protocols. MS mobility events are signaled to the scheduling service to control migration of existing active data connections to neighboring BSs, and to initiate adaptations in the global routing protocol. The scheduling solution exploits spectral reuse using the initial centralized scheduling scheme and supports traffic load fluctuations using the borrowing mechanism proposed by the distributed adaptation.

The network throughput performance per routing zone using a centralized

only scheduling approach and an approach that uses an initial centralized scheduling scheme with distributed adaptation was presented. An analytical model for chain and single intersection topology was derived to identify the increase in overall network throughput per routing zone using the distributed adaptation approach. It was determined that the increase in overall network throughput is not significant in dense network scenarios where each base station has enough subscriber stations to use up all of its allocated bandwidth on the mesh link. Ns-2 simulations verified the analytical model and an increase of 8.2% in overall network throughput was obtained for a typical dense network scenario. On the other hand, the increase in overall network throughput is quite significant for sparse network scenarios where each base station has plenty of data slots it can lend to the requesting base stations. Through ns-2 simulations, it was shown that the increase in overall network throughput can reach as high as 232% for a typical sparse network scenario.

7.2 Future Work

As mentioned in Chapter 6, analysis for the grid topology has not been performed yet and remains a topic of future work. Computer aided simulations and concepts such as linear programming are going to be used to study the analysis. Also, the borrowing scheme considered in this thesis only allows base stations to borrow from immediate (1-hop) neighbors. The performance of allowing multi-hop borrowing scheme also remains a topic of future work.

Appendix

Simulator Setup

The proposed scheduling solution was implemented as extensions to the network simulator ns-2 and the NIST IEEE 802.16 extension (04-30-2007 release) [26]. The NIST extension models the IEEE 802.16-2004 PMP mode with a single static bandwidth allocation scheme, and the IEEE 802.16e-2005 standard handover. An overview of the IEEE 802.16-2004 implementation in ns-2 is provided in Figure A.1. QoS support using service flow architecture as depicted in Figure A.2 is added to the IEEE 802.16-2004 MAC implementation. All BSs and MSs are simulated using the NIST 802.16 node model extended with models of mesh mode operation and BS-supported handover.

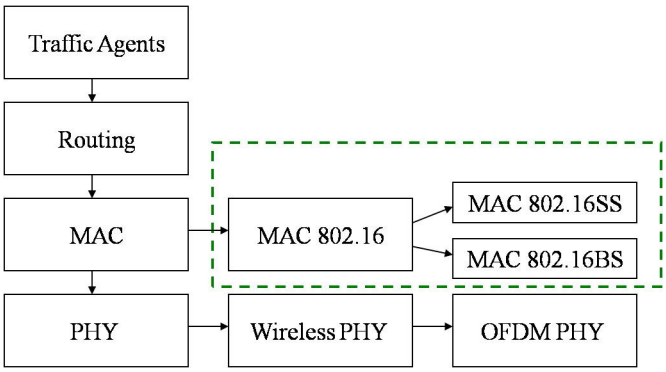

Figure A.1: IEEE 802.16-2004 implementation in ns-2

A TDMA based wired-link connection is implemented to simulate the mesh mode OFDM modulation operating in TDD mode with dynamically controllable

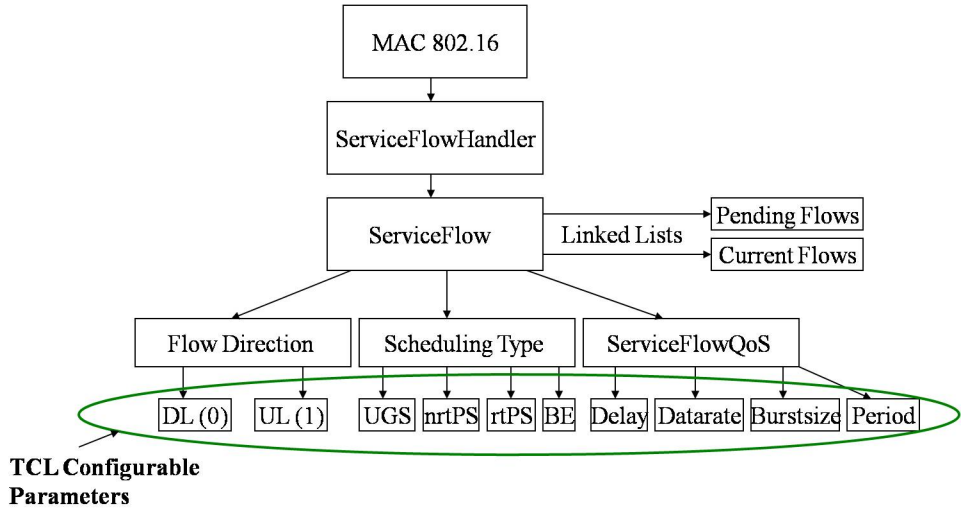

Figure A.2: QoS Service Flow implementation hierarchy

transmission schedules. The mesh radio is assumed to be operating on a 10 MHz channel and using OFDM_64QAM_3_4 modulation scheme. This results in a maximum theoretical throughput of 19 Mbps per mesh link. The mesh frame size is selected to be 10 milliseconds. This results in a throughput of 190000 bits/frame. When operating at OFDM_64QAM_3_4, one OFDM symbol consists of 856 bits. Thus, the number of OFDM symbols per frame is 190000/856 = 221 symbols.

The mesh frame structure reserves 7*MSH_CTRL_LEN OFDM symbols for control sub-frame. MSH_CTRL_LEN represents the number of nodes that are part of the mesh.In the chain topology scenario, 7 BSs (MSS 1' - MSS 3', MBS, MSS 1 - MSS 3) are part of the mesh and so 7*MSH_CTRL_LEN = 49 OFDM symbols are reserved in each Mesh frame for the control sub-frame. So, the data sub-frame is made up of 221 - 49 =172 OFDM symbols. Each symbol is simulated to be a mini-slot. So, 172 data slots have to be allocated per frame for the mesh schedule.

Bibliography

[1] IEEE. IEEE standard for local and metropolitan area networks part 16: Air interface for fixed broadband wireless access systems. In *IEEE Std 802.16-2004*, 2004.

[2] IEEE. IEEE standard for local and metropolitan area networks part 16: Air interface for fixed and mobile broadband wireless access systems. In *IEEE Std 802.16-2005*, 2005.

[3] Army Technology. Us army's cerdec to evaluate wibro. http://www.army-technology.com/news/news1298.html, 2007.

[4] Nortel Networks. News release: Nortel demonstrates commitment to leadership in 4g mobile broadband. http://www.nortel.com/news, 2006.

[5] K. Wongthavarawat and A. Ganz. IEEE 802.16 based last mile broadband wireless military networks with quality of service support. In *IEEE MILCOM*, volume 2, pages 779–784, October 2003.

[6] B.K. Hartzog and T.X. Brown. WiMAX - potential commercial off-the-shelf solution for tactical mobile mesh communications. In *IEEE MILCOM*, pages 1–7, October 2006.

[7] M. Sherman, K.M. McNeill, K. Conner, P. Khuu, and T. McNevin. A PMP-friendly MANET networking approach for WiMAX/IEEE 802.16. In *IEEE MILCOM*, pages 1–7, October 2006.

[8] B. Bennett and P. Hemmings. Operational considerations of deploying WiMAX technology as a last-mile tactical communication system. In *IEEE MILCOM*, pages 1–7, October 2006.

[9] H. Wei, S. Ganguly, R. Izmailov, and Z. Haas. Interference-aware IEEE 802.16 WiMAX mesh networks. In *IEEE VTC*, volume 5, pages 3102–3106, 2005.

[10] Liu Zhe, Zhigiang He, Weiling Wu, and Xinglin Wang. A simplified layered qos scheduling scheme in ofdm networks. In *IEEE VTC*, pages 1842–1846, October 2007.

[11] C. Schwingenschlogl, V. Dastis, P.S. Mogre, M. Hollick, and R. Steinmetz. Performance analysis of the real-time capabilities of coordinated centralized scheduling in 802.16 mesh mode. In *IEEE VTC*, volume 3, pages 1241–1245, 2006.

[12] M.S. Kuran, B. Yilmaz, F. Alagoz, and T. Tugcu. Quality of service in mesh mode IEEE 802.16 networks. In *SoftCOM*, pages 107–111, 2006.

[13] M. Cao, W. Ma, Q. Xhang, and X. Wang. Analysis of IEEE 802.16 mesh mode scheduler performance. In *IEEE Transactions on Wireless Communications*, volume 6, pages 1455–1464, 2007.

[14] Y. Lebrun, F. Horlin, A. Bourdoux, and L. Van der Perre. Feasibility study of the mesh extension for the IEEE 802.16e communication system. In *IEEE VTC*, pages 93–96, 2006.

[15] J. Andrews, A. Ghosh, and R. Muhamed. *Fundamentals of WiMAX*. NJ: Prentice-Hall, 2007.

[16] Lien-Wu Chen, Yu-Chee Tseng, Da-Wei Wang, and Jan-Jan Wu. Exploiting spectral reuse in resource allocation, scheduling, and routing for IEEE 802.16 mesh networks. In *IEEE VTC*, pages 1608–1612, October 2007.

[17] Xiong Qing, Jia Weijia, and Wu Chanle. Packet scheduling using bidirectional concurrent transmission in WiMAX mesh networks. In *WiCOM*, pages 2037–2040, September 2007.

[18] R. Jayaparvathy, G. Sureshkumar, and P. Kanakasabapathy. Performance evaluation of scheduling schemes for fixed broadband wireless access systems. In *IEEE Network*, volume 2, pages 16–18, 2005.

[19] A. Lera, A. Molinaro, and S. Pizzi. Channel-aware scheduling for QoS and fairness provisioning in IEEE 802.16/WiMAX broadband wireless access systems. In *IEEE Network*, volume 21, pages 34–41, 2007.

[20] J.-C. Lin, C.-L. Chou, and C.-H. Liu. Performance evaluation for scheduling algorithms in WiMAX network. In *Advanced Information Networking and Applications Workshops*, pages 68–74, 2008.

[21] A. Bacioccola, C. Cicconetti, A. Erta, L. Lenzini, and E. Mingozzi. Bandwidth allocation with half-duplex stations in IEEE 802.16 wireless networks. In *IEEE Transactions on Mobile Computing*, volume 6, pages 1384–1397, 2007.

[22] D. Niyato and E. Hossain. Queue-aware uplink bandwidth allocation and rate control for polling service in IEEE 802.16 broadband wireless networks. In *IEEE Transactions on Mobile Computing*, pages 668–697, 2006.

[23] C. Cicconetti, L. Lenzini, E. Mingozzi, and C. Eklund. Quality of service support in IEEE 802.16 networks. In *IEEE Network*, volume 20, pages 50–55, 2006.

[24] C. Cicconetti, A. Erta, L. Lenzini, and E. Mingozzi. Performance evaluation of the IEEE 802.16 MAC for QoS support. In *IEEE Transactions on Mobile Computing*, volume 6, pages 26–38, 2007.

[25] IETF. RFC 2002 - ip mobility support. http://www.ietf.org/rfc/rfc2002.txt, 1996.

[26] NIST. Seamless and security project: Software tools. http://w3.antd.nist.gov/seamlessandsecure.shtml, 2007.